

Review

Recent advances in nanomedicines for photodynamic therapy (PDT)-driven cancer immunotherapy

Bin Ji^{1,2}, Minjie Wei^{1✉}, Bin Yang^{1,2✉}

1. School of Pharmacy, China Medical University, Shenyang, Liaoning 110122, China.

2. The First Affiliated Hospital, China Medical University, Shenyang, Liaoning 110001, China.

✉ Corresponding authors: Minjie Wei, Ph.D. and Bin Yang, Dr. Tel: +86-24-83283177; Fax: +86-24-83283177. E-mail: mjwei@mail.cmu.edu.cn; binyang@cmu.edu.cn.

© The author(s). This is an open access article distributed under the terms of the Creative Commons Attribution License (<https://creativecommons.org/licenses/by/4.0/>). See <http://ivyspring.com/terms> for full terms and conditions.

Received: 2021.09.20; Accepted: 2021.10.27; Published: 2022.01.01

Abstract

Cancer immunotherapy has made tremendous clinical progress in advanced-stage malignancies. However, patients with various tumors exhibit a low response rate to immunotherapy because of a powerful immunosuppressive tumor microenvironment (TME) and insufficient immunogenicity of tumors. Photodynamic therapy (PDT) can not only directly kill tumor cells, but also elicit immunogenic cell death (ICD), providing antitumor immunity. Unfortunately, limitations from the inherent nature and complex TME significantly reduce the efficiency of PDT. Recently, smart nanomedicine-based strategies could subtly modulate the pharmacokinetics of therapeutic compounds and the TME to optimize both PDT and immunotherapy, resulting in an improved antitumor effect. Here, the emerging nanomedicines for PDT-driven cancer immunotherapy are reviewed, including hypoxia-reversed nanomedicines, nanosized metal–organic frameworks, and subcellular targeted nanoparticles (NPs). Moreover, we highlight the synergistic nanotherapeutics used to amplify immune responses combined with immunotherapy against tumors. Lastly, the challenges and future expectations in the field of PDT-driven cancer immunotherapy are discussed.

Key words: cancer immunotherapy; immune response; photodynamic therapy; emerging nanomedicines; synergistic nanotherapeutics

1. Introduction

Conventional antitumor therapies including surgical resection, chemotherapy, radiotherapy, and molecular targeted therapy are used to effectively treat the early-stage tumors, while they are still helpless for advanced-stage disease [1]. Encouragingly, cancer immunotherapy could prevent the recurrence of cancer and prolong the survival times of end-stage patients by activating the hosts' immune system [2]. So far, numerous immune-based therapies have been approved for cancer treatment, such as checkpoint blockade immunotherapy, adoptive cell therapy (ACT), and cancer vaccines [3-6]. Among these therapies, immune checkpoint therapy has successfully shifted the clinical research landscape. For example, the first FDA approved checkpoint inhibitor, therapeutic antibody

ipilimumab, was used to block cytotoxic T lymphocytes (CTL) A-4, leading to a prominent regression of metastatic melanoma [7]. Additionally, treatment with PD-1 blocking antibodies (e.g., nivolumab) significantly improved the objective response rate in many advanced cancers [8].

Despite the aforementioned benefits of immune checkpoint therapy, a large number of patients with various cancers are not sensitive to immune checkpoint inhibitors due to their low tumor immunogenicity [9-11]. When a photosensitizer (PS) absorbs a photon of light, it can experience the following three different fates: First, the PS is activated from the ground state to a short-lived excited singlet state, and then the excited PS may decay back to the ground state by emitting

fluorescence. Second, the abovementioned short-lived excited singlet state of the PS may undergo intersystem crossing to form a relatively long-lived triplet state. The triplet excited PS can interact with some endogenous substances to form a free radical (e.g., H₂O₂ and O₂⁻). Alternatively, the relatively long-lived triplet state can directly interact with molecular oxygen to form ¹O₂. In most cases, the ROS generated by PS in PDT mainly refers to the last process [12, 13]. Recently, PSs activated by local laser irradiation induced PDT and selectively damaged the tumor tissue instead of normal organs [14-17]. Compared to surgery, PDT is less invasive. More importantly, several studies have confirmed that PDT also stimulated antitumor immune response through a variety of mechanisms [18]. Some examples are as follows: 1) Calreticulin (CRT), located on the endoplasmic reticulum (ER), moves to the cell membrane's surface undergoing PDT and provides an "eat me" signal to cause an immune response [19]. 2) Upregulation of transcription factor expression (NF-κB), protein (heat shock protein 70) [20], or promoting secretion of cytokines (IFN-γ, IFN-α) [21]. 3) Promoting mutations of antigen presenting cells (APCs) and CTLs to homing [22]. 4) Recruitment of neutrophils to kill cancer cells and then causing the infiltration of macrophages [23, 24]. Among them, PS-generated PDT can excellently initiate an immunogenic cell death (ICD), which is the most commonly used methods to induce immune response. With the progress of ICD, tumor cells show sequential changes [24]. For instance, CRT and heat shock proteins (HSPs) will be exposed on the surface of dying cells. Adenosine triphosphate (ATP) and high-mobility group box 1 protein (HMGB1) will be released from the dying cells. The released ATP drives the APCs into tumor bed. The exposure of CRT facilitates the incorporation of APCs to phagocytose dead cells. The released HMGB1 promotes the TAA presentation to APCs. The maturation and migration of DCs is mediated by the expression of HSPs. In addition, the ICD can further boost the APC maturation via secreting proinflammatory cytokines. Therefore, the ICD can significantly facilitate the activation of immune response. More importantly, the ICD effectively serves as a bridge to connect the PDT with immunotherapy for cancer treatment [24, 25].

However, several factors significantly limit the efficacy of PDT, which further reduces their capability to induce immune response. First, tumor hypoxia can weaken the efficacy of oxygen-dependent PDT, and the oxygen consumption of PDT will further aggravate tumor hypoxia, leading to a vicious circle

[26]. Second, most PSs are activated by a short-wavelength light (400-700 nm), significantly hindering PDT for the treatment of deep-seated tumors due to the inferior tissue penetration ability of specific light [27]. Third, PSs in high concentrations usually cause aggregation-caused quenching (ACQ), which will deeply weaken the optical property of PSs [28]. Fourth, systemic administration of PSs might cause phototoxicity due to off-target distribution and accumulation in normal tissues [29, 30].

Fortunately, advanced nanomedicines have opened new promising avenues to refine and improve the performance of PDT, leading to an enhanced immune response [31]. Advanced nanomedicines can solve the tumor hypoxia problem by combining various self-supply oxygen strategies. Using emerging nanocarriers, nanomedicines can control the *in vivo* distribution of PSs to achieve tumor-targeting accumulation. In addition, smart tumor microenvironment (TME)-responsive nanoplates not only reduce phototoxicity by avoiding the premature leakage of PS in blood circulation, but also accelerate the release of PSs to overcome the ACQ effect at the tumor site. More importantly, nanomedicines excellently codeliver PSs and immunomodulators to their targets, resulting in an optimal cancer immunotherapy. Herein, we review the emerging nanomedicines for PDT-driven cancer immunotherapy. Moreover, we highlight the synergistic nanotherapeutics for increasing immune responses combined with immunotherapy against tumors (**Figure 1**). Finally, the current challenges and future perspectives in the field of PDT-driven cancer immunotherapy are also highlighted.

2. Emerging nanomedicines for PDT-driven cancer immunotherapy

Conventional immunotherapies are usually unable to transform nonimmunogenic (cold) tumors into immunogenic (hot) tumors [32, 33]. Encouragingly, nanomedicine-based therapeutic strategies have the capability to transform cold into hot tumors, especially for aforementioned PDT with several immunostimulatory mechanisms to initiate the immune response [34, 35]. Recently, advanced nanomedicines have been designed to improve the efficacy of PDT, including tumor hypoxia-reversed nanomedicines, TME-responsive NPs, upconversion NPs (UCNs), and nanosized metal-organic frameworks (nMOFs). The optimized PDT combined with immunotherapy would achieve a strong synergistic effect against advanced cancers.

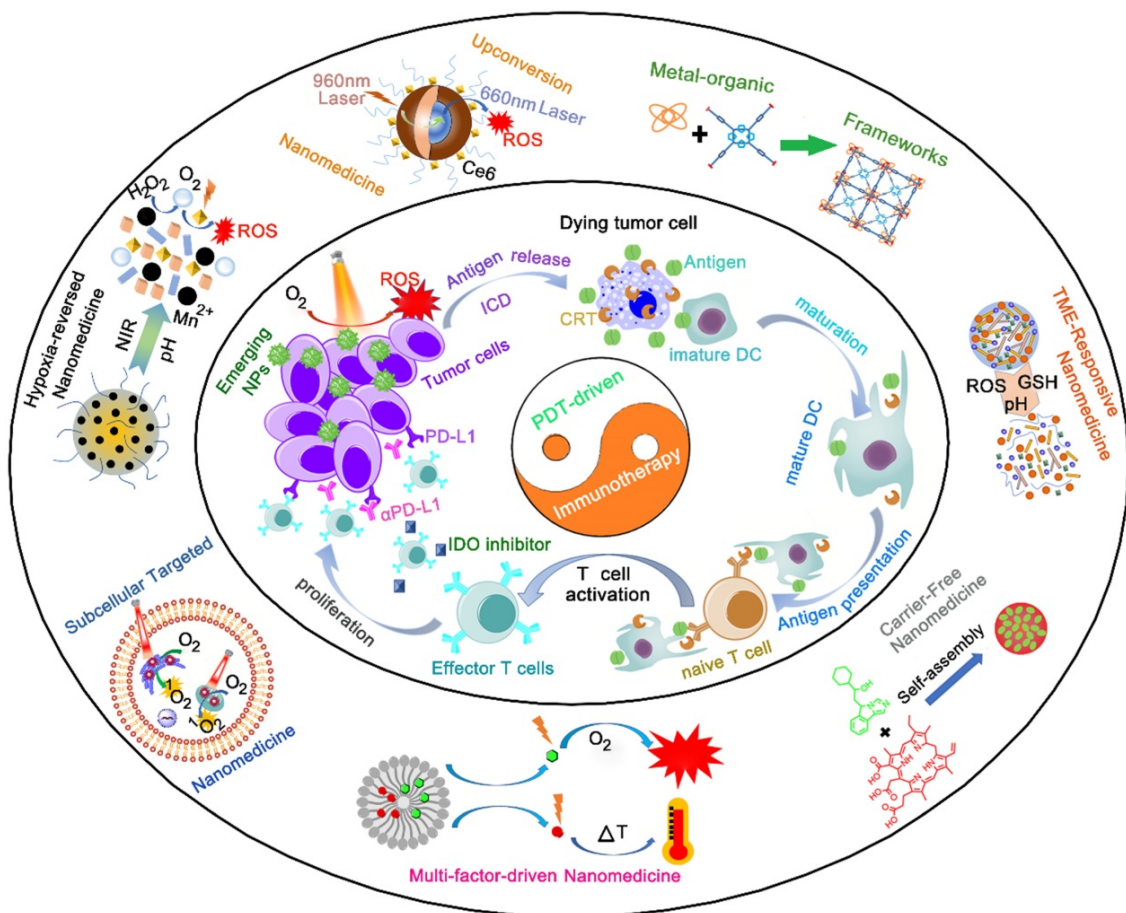


Figure 1. Schematic illustration of emerging nanomedicines for PDT-driven cancer immunotherapy. The outer shell shows recent nanomedicines developed for PDT-driven cancer immunotherapy, including tumor hypoxia-reversed nanomedicines, UCNs, nanosized nMOFs, TME-responsive NPs, subcellular targeted NPs, carrier-free and small-molecule prodrug-based self-assembled NPs, and multifactor-driven nanomedicines. The inner core explains how to amplify the combination of PDT and immunotherapy, thereby improving the effect of cancer treatment.

2.1. Tumor hypoxia-reversed nanomedicines for PDT-driven cancer immunotherapy

Rapid tumor growth causing insufficient blood supply and local oxygen consumption of PDT aggravates tumor hypoxia, seriously affecting the efficacy of PDT [36, 37]. In addition, tumor hypoxia can suppress antitumor immunity by facilitating the proliferation of immunosuppressive cells (e.g., M2 type macrophages) to promote tumor development and recurrence [38-40]. Hence, alleviating hypoxia in the tumor site is an important method to improve the efficacy of PDT-driven cancer immunotherapy. Recently, researchers developed various biomaterials and therapeutic agents to alleviate tumor hypoxia, including hemoglobin, catalase (CAT), manganese dioxide NPs, oxygen-shuttle nanoperfluorocarbon (nanoPFC), hyaluronidase (HAase), and metformin (Met) (Table 1) [41-46].

2.1.1. H₂O₂-activated oxygen-producing NPs (HAOP NPs) for PDT-driven cancer immunotherapy

Nowadays, some inorganic biomaterials (e.g.,

manganese dioxide (MnO_2)) can activate hydrogen peroxide overexpressed in tumor cells to produce oxygen [47]. Therefore, HAOP NPs can be used to solve the problem of tumor hypoxia. Furthermore, gold nanocages (AuNCs) mediated ROS production as intrinsic inorganic PSs, and gold-based nanomedicines can improve the PDT efficiency of other PSs owing to a localized electric field (LEF) [48, 49]. Based on these theories, Liang et al. designed a TME-responsive core-shell AuNC@ MnO_2 (AM) nanoplateform for oxygen-boosted PDT combined with immunotherapy against metastatic breast cancer (Figure 2A) [41]. Under acidic TME conditions, the MnO_2 shell degrades and catalyzes the reaction of intracellular H_2O_2 to produce abundant oxygen, and then the self-generated O₂ further improved the ROS production of AM upon light irradiation by ameliorating tumor hypoxia. More importantly, the oxygen-boosted PDT robustly induced more powerful ICD compared with the PDT caused by AuNCs, thereby enhancing the antitumor immune response. As a result, this oxygen-boosted AM nanoplateform not only effectively inhibited the local tumor growth

but also prevented the tumor metastases [41, 50]. However, gold-based nanomedicines cause some problems for the organism, including difficulty in degradation or excretion, a potential toxic effect [51]. Fortunately, recent studies showed that biodegradable $\text{CaCO}_3/\text{MnO}_2$ -based nanocarriers can be used to deliver therapeutic cargos and serve as contrast agents [42]. Moreover, this type of nanocarriers can be responsive to TME and modulate it. For instance, Liu et al. designed a TME-responsive biodegradable nanoplateform by combining PDT and immune checkpoint therapy for improving cancer treatment. This biodegradable nanoplateform ($\text{Mn}@\text{CaCO}_3/\text{ICG}@\text{siRNA}$) was constructed from MnO_2 NPs covered with an ICG-doped acid-sensitive layer of CaCO_3 and loaded with PD-L1-targeting siRNA through electrostatic interaction [42]. After reaching the acidic TME, the layer of CaCO_3 was rapidly decomposed into CO_2 and Ca^{2+} (biological components), and subsequently the core of MnO_2 NPs triggered the reaction of tumor intracellular H_2O_2 to produce H_2O and O_2 , which not only reversed the tumor hypoxia but also provided the necessary elements of PDT (O_2). Compared with free ICG, $\text{Mn}@\text{CaCO}_3/\text{ICG}@\text{siRNA}$ produced much more ${}^1\text{O}_2$ owing to the MnO_2 -mediated HAOP NPs, thereby significantly improving the efficacy of PDT. More importantly, a combination of PDT and siRNA provided synergistic benefits by enhancing the tumor immunogenicity via PDT and silencing the PD-L1 gene by siRNA, thus leading to a powerful antitumor efficiency.

In addition to MnO_2 NPs, CAT, an endogenous antioxidant enzyme, also efficiently triggered the decomposition of tumor intracellular H_2O_2 to generate O_2 for relieving tumor hypoxia, thus increasing the anticancer efficacy of PDT and remodeling the immunosuppressive TME [52, 53]. For instance, Jiang et al. developed an oxygen-producing phototherapy hydrogel (POP-Gel) to inhibit the proliferation and metastasis of breast cancer (**Figure 2B**). In this study, they fabricated hydrogel scaffolds using FDA-approved Pluronic® F127 and F68, which is

loaded with Ce6 as the PS and CAT assisted by CaO_2 as a catalyst to continuously supply oxygen for a long time to alleviate tumor hypoxia [52]. With immunofluorescence staining and photoacoustic (PA) imaging, they showed that the oxygen generated using this platform could be prolonged for up to five days, thereby realizing the strategy ("once injection, sustained treatment"). As a result, the hypoxic regions of tumors were reduced, thus significantly improving the PDT efficacy and decreasing the expression of hypoxia-related factors. Furthermore, the improved PDT induced an extreme immune response, enhancing the inhibition of cancer growth.

Although the oxygen-producing phototherapy nanoplateform effectively enhanced the post-PDT-triggered immune response, the immunosuppressive TME hindered the ultimate efficacy of PDT-mediated cancer immunotherapy by suppressing the activation of CTLs [54]. To overcome these hurdles, Liu et al. reported a synergistic treatment strategy by utilizing oxygen-boosted PDT combined with checkpoint blockade therapy for eliminating metastatic tumors [54]. First, they designed a light-triggered hydrogel composed of Ce6 modified CAT, biodegradable polymer (poly(ethylene glycol) double acrylate, termed as PEGDA), and immune adjuvant (R837-loaded PLGA NPs). After the intratumor injection of precursor solution upon laser irradiation, the polymeric matrix helped in the polymerization of PEGDA by ROS to form *in situ* gelation, thus retaining various agents (Ce6-CAT and immune adjuvant). Subsequently, Ce6-CAT by repeated laser stimulation continuously generated ROS to induce strong ICD and regulate the polarization of macrophage, as the retained CAT could overcome tumor hypoxia by persistently producing O_2 . Furthermore, the PDT-mediated ICD, along with the immune adjuvant, would induce a significantly enhanced immune response [54]. More importantly, application of α -CTLA4 blockade therapy significantly suppressed the activation of Treg, further improving the multiround PDT-mediated immunotherapy.

Table 1. Summary of emerging tumor hypoxia-reversed nanomedicines for PDT-driven cancer immunotherapy. (\uparrow = upregulation, \downarrow = downregulation).

Formulations	Therapeutic agents	Immunologic modulation	Ref
AuNC@ MnO_2 NPs	AuNCs, MnO_2	TAAs, mDC, CD4 $^+$, CD8 $^+$, NK \uparrow	41
$\text{Mn}@\text{CaCO}_3/\text{ICG}@\text{siRNA}$ NPs	ICG, MnO_2 , siRNA	TAAs, mDC, IL12, IL18, CD4 $^+$, CD8 $^+$, INF- γ \uparrow PD-L1 \downarrow	42
Phototherapy hydrogel	Ce6, CAT	TAAs, mDC, CD4 $^+$, CD8 $^+$ \uparrow HIF-1 α , VEGF \downarrow	52
R837-loaded PLGA NPs	Ce6, CAT, α -CTLA4	TAAs, mDC, CD4 $^+$, CD8 $^+$ \uparrow CTLA-4 \downarrow	54
HSA/Hb NPs	Ce6	TAAs, mDC, CD4 $^+$, CD8 $^+$, NK \uparrow	43
ICG modified gold nanospheres	ICG,	TAAs, mDC, CD4 $^+$, CD8 $^+$ \uparrow	57
Fluorinated polymer NPs	Ce6, NLG919	TAAs, mDC, CD4 $^+$, CD8 $^+$, Trp \uparrow Kyn \downarrow	44
DEX-HAase NPs	Ce6, HAase, α -PD-L1	TAAs, mDC, CTLs, INF- γ , M1 macrophage \uparrow M2, PD-L1 \downarrow	45
HPR@CCP NPs	Ce6, HAase, Cas9-Ptpn2 plasmids	TAAs, mDC, CD8 $^+$, INF- γ , TNF- α \uparrow	62
PM-IR780-Met NPs	IR780, Met	TAAs, mDC, CTLs \uparrow Tregs, MDSC \downarrow	46
IR775@Met@Liposomes	IR775, Met	TAAs, mDC, CTLs, INF- γ \uparrow , PD-L1 \downarrow	63

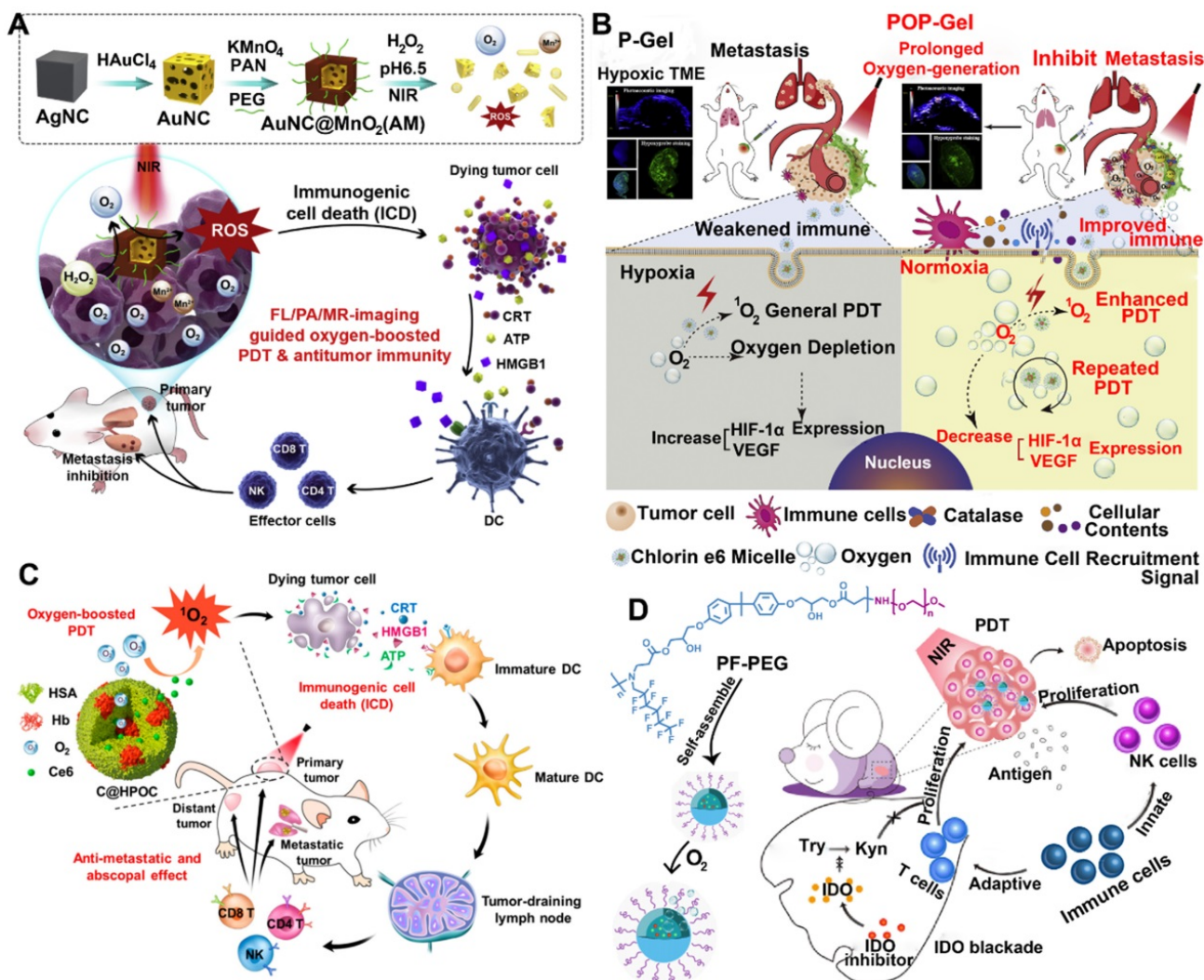


Figure 2. Schematic illustration of various tumor hypoxia-reversed nanomedicines for PDT-driven cancer immunotherapy. (A) AuNC@MnO₂ (AM) NPs, (B) Oxygen-producing phototherapy hydrogel (POP-Gel), (C) Ce6@Oxygen-carrying hybrid protein NPs, (D) Oxygen-carrying fluorinated polymer NPs (FPNs). Reproduced with permission [41, 43, 44, 52]. Copyright 2018, Elsevier Ltd; Copyright 2019, Elsevier Ltd; Copyright 2018, American Chemical Society; Copyright 2019, Elsevier Ltd.

2.1.2. Oxygen-carrying NPs for PDT-driven cancer immunotherapy

In hypoxic solid tumors, the efficacy of PDT is largely reduced by hypoxia. To overcome this challenge, many efforts have been made to decompose H₂O₂ to supply O₂. However, the H₂O₂ levels in some parts of the tumor are very low, and the results are significantly limited [55, 56]. Fortunately, some studies have shown that hemoglobin, red blood cells, and PFC carry O₂ directly to hypoxic tumors [43, 44]. Chen et al. designed a hybrid protein oxygen nanocarrier with Ce6 for oxygen self-sufficient PDT and achieved cancer immunotherapy (**Figure 2C**) [43]. This hybrid protein oxygen nanocarrier is composed of hemoglobin (Hb) and human serum albumin (HSA). This is because the excellent oxygen-transport carrier (free Hb) has a short circulation time and poor stability, while HSA exhibits good *in vivo* stability and

biocompatibility [43]. This hybrid protein oxygen nanocarrier can significantly reduce tumor hypoxia by simultaneously codelivering the PS and oxygen to the tumor, thereby significantly improving the effect of PDT and the infiltration of CD8⁺ T cells at the tumor site. More importantly, the increased PDT induced a strong ICD by improving the release amount of damage-associated molecular patterns (DAMPs) to activate more dendritic cells (DCs), NK cells, and CTLs, thus effectively inhibiting the primary tumors and suppressing lung metastasis [43]. Similarly, a recent study developed auxiliary liposomes loaded with oxygen-laden Hb to enhance the efficacy of PDT caused by ICG modified gold nanospheres [57]. After the liposomes loaded with oxygen-laden Hb reached the tumor hypoxia condition, the oxygen was rapidly released from the Hb, assisting the ICG to generate robust ROS, thus improving the intensity of immune response.

Aside from Hb, PFCs can store O₂ molecules like a reservoir, as PFCs have weak intermolecular cohesive forces to boost the insertion of oxygen molecules [58]. Xing et al. developed a versatile nanosystem consisting of fluorinated polymer NPs (FPNs) with the simultaneous encapsulation of NLG919 and Ce6 for improving the efficacy of PDT and modulating immunosuppressive TME (**Figure 2D**) [44]. Compared to alkylated polymer NPs, FPNs showed high oxygen carrying capacity, thereby generating much more ROS and treating hypoxic tumor. Meanwhile, the enhanced PDT and remodeled TME also induced increased immunological responses and promoted the proliferation of CTLs. More importantly, a combination of indoleamine 2,3-dioxygenase (IDO) blockade therapy and PDT achieved more effective antitumor results compared with PDT alone, as the encapsulated NLG919 inhibited the IDO pathway, thus restoring the activation of CTLs [44].

2.1.3. ECM-degraded and respiration-inhibited NPs for PDT-driven cancer immunotherapy

The TME contains an abnormally condensed extracellular matrix (ECM), which not only reduces the oxygen supply via squeezing the tumor blood vessels but also impedes the diffusion of oxygen by serving as a physical barrier [59-61]. The dense ECM is composed of some glycosaminoglycan, proteins, etc., among which the cross-linked hyaluronic acid (HA) plays an important role in forming the physical barrier [45, 61]. HAase is a specifical enzyme to hydrolyze HA. Hence, the application of HAase to decompose HA is a promising strategy to relieve tumor hypoxia [45]. For instance, Wang et al. designed a cascade delivery strategy for improving the TME and enhancing PDT-mediated cancer immunotherapy [45]. First, they developed a natural biocompatible polymer nanoparticle system via the self-assembly of dextran-modified HAase (DEX-HAase) by inserting pH-responsive linkers. Compared to free HAase, the DEX-HAase NPs significantly improved the stability of HAase in blood circulation. Furthermore, because of the presence of pH-responsive linkers, the DEX-HAase NPs selectively triggered the release of HAase to decompose the HA after accumulating in the acidic TME, loosening the condensed ECM [45]. The loosened tumor ECM further increased the penetration of oxygen molecules to relieve tumor hypoxia and reverse the immunosuppressive TME. After the first wave injection of DEX-HAase NPs, the remodeled TME enhanced the efficacy of PDT caused by the second wave injection of Ce6@liposome plus irradiation [45]. More importantly, the enhanced PDT

induced an intense immune response, and the PDT-mediated cancer immunotherapy was further improved by combining with PD-L1 blockade therapy after injecting the third wave of anti-PD-L1. As a result, this sequential injection of therapeutic agents achieved cooperative PDT-immunotherapy, effectively inhibiting the growth of primary tumor as well as distant tumor [45].

Apart from anti-PD-L1, clustered regularly interspaced short palindromic repeats associated protein 9 (CRISPR-Cas9) could effectively damage the protein tyrosine phosphatase nonreceptor type 2 (Ptpn2) gene, resulting in the enhanced activation of CD8⁺ T cells. For example, Qian et al. designed a core-shell nanosystem to achieve a combined photodynamic-immunotherapy, in which the core is composed of modified PSs and Cas9-Ptpn2 plasmids [62]. With the administration of HAase in advance, both the HA shell of the nanosystem and the HA shell in tumor ECM were degraded, thus improving the penetration of loading cargos and O₂. Therefore, this nanosystem under laser irradiation could trigger an enhanced PDT because of the alleviated hypoxia to induce a strong immune response. Furthermore, the Cas9-Ptpn2 plasmids in this nanosystem were developed to damage the Ptpn2 gene, leading to increasing proliferation of T lymphocytes and secretion of cytokines (IFN- γ , IFN- α) [62].

The inhibition of respiration could decrease the oxygen consumption of tumor cells, which offers an indirect way to enhance the supply of oxygen for PDT. Recently, many studies reported that Met could decrease oxygen consumption by inhibiting mitochondrial respiratory chain [46, 63]. For example, Teng et al. constructed a platelet-mimicking nanoparticle system composed of Met and PS (IR780) to integrate immunosuppressive reversion and immunogenic activation. In this study, IR780 could initiate an oxygen-boosted PDT with the help of Met-mediated mitochondrial respiration inhibition, resulting in an ICD-based immunogenic activation. Moreover, the alleviated tumor hypoxia by reducing oxygen consumption weakened the immunosuppression mediated by myeloid-derived suppressor cells (MDSC) [46]. In another study, Shen et al. developed a multifunctional liposome coloaded with IR775 and Met. They found that Met not only reversed tumor hypoxia to enhance IR775-induced PDT, but also regulated the endoplasmic-reticulum-associated degradation by pAMPK pathway to reduce the PD-L1 expression [63].

2.2. UCNs for PDT-driven cancer immunotherapy

Most PSs for PDT are activated by a short

wavelength (e.g., visible light), leading to a limited penetration depth in live tissues. Furthermore, the chromosomes (hemoglobin, etc.) of organization can strongly absorb visible light, significantly interfering with the PS on the transformation of light [64–66]. Therefore, the efficacy of PDT with the depth of tissue significantly reduced, resulting in incomplete treatment and recurrence. To find an effective method to overcome the depth of tissue penetration has become an urgent need to solve the problems of PDT at this stage.

UCNs are nanometer-sized materials that convert low-energy light to high-energy light through sequential excitation with multiple photons via an anti-Stokes emission process. Compared with downconverted NPs, UCNs can absorb near-infrared (NIR) light and have a relatively high depth of tissue penetration, while the light can be converted into strong UV or visible light [12, 66]. Based on this feature, UCN-based PDTs have been extensively studied for tumor therapy to improve the tissue penetration depth. For example, Ai et al. constructed Ce6-loaded UCNs combined with HA plus MnO₂ nanosheets to improve NIR light-mediated PDT [67]. The Ce6-loaded UCNs could be efficiently activated to generate sufficient ¹O₂ for inducing both deep-tissue cellular ablation by converting 808 nm light excitation into 655 nm emissions. Furthermore, the surface-anchored HA significantly inhibited the tumor recurrence post-PDT treatment by producing M1-type macrophages instead of M2-type macrophages.

In addition to M1-type macrophages, the CD8⁺ T cells also play an important role in preventing tumor recurrence. However, the activation of CD8⁺ T cells was suppressed by regulatory T cells (T_{reg}) [68]. Fortunately, several studies have reported that the activity of T_{reg} cells was effectively inhibited by checkpoint blockade (e.g., anti-CTLA-4 antibody) [68, 69]. For instance, Xu et al. designed a multitasking nanoplatform composed of UCNs as an NIR-responsive vehicle, imiquimod (R837) as an immune adjuvant, and Ce6 as a PS (**Figure 3**) [68]. The UCN-based platform overcame limited penetration depth by the application of NIR irradiation, thus triggering the loaded Ce6 to generate ROS. Subsequently, the generated ROS further destructed the tumor cells to produce numerous tumor-associated antigens (TAAs) accompanied by the loaded immune adjuvant (R837) to provide powerful immune responses. More importantly, the powerful immune responses caused by UCN-Ce6-R837-based PDT was further improved by using anti-CTLA-4 antibodies, which suppress the vitality of Treg cells, thus restoring the activity of

CTLs. As a result, the abovementioned synergistic treatment strategy not only eliminated the distant tumors, but also showed prolonged immune memory effect and inhibited the tumor recurrence.

2.3. Nanosized nMOFs for PDT-driven cancer immunotherapy

During PDT, a high concentration of PSs in a tight core of NPs often causes ACQ effect, causing a reduced yield of ROS and self-quenching fluorescence [70, 71]. Unlike the PS-loaded nanomedicines, nMOFs based on the incorporation of PSs as construction units have tunable and porous structures that overcome the ACQ effect and endow high PS loadings [70, 72]. Furthermore, the porous structures of nMOFs can not only well disperse the PSs, but also facilitate the diffusion of ROS, thereby enhancing the efficacy of PDT [70]. For instance, Cai et al. designed *in situ* tumor vaccines, consisting of MOF-based NPs (PCNs), immunologic adjuvant (CpG), and hypoxia-inducible factor inhibitor (acriflavine) [73]. To achieve excellent tumor-targeting capacity, they coated the surface of PCN-CpG-acriflavine with HA to recognize the CD44 receptor overexpressed on tumor cell surface. In their study, the self-assembled PCNs were composed of zirconium ions and H₂TCPP, and the well-dispersed H₂TCPP in its framework induced a comparable PDT by overcoming the ACQ effect. Furthermore, the PCNs loaded with acriflavine suppressed the enhanced hypoxic signaling caused by PDT, thereby reversing the tumor hypoxia. More importantly, the PDT-generated TAAs combined with CpG achieved a synergistic effect to provide intensive immune responses [73]. To further improve the immune response, Zhang et al. developed a fusion cytomembrane (FM)-coated nMOF for photo-activatable cancer immunotherapy, where the FMs were derived from DCs and tumor cells [74]. In their study, the FMs not only showed an excellent tumor-targeting capacity because of the self-targeting characteristic to homologous tumors, but also facilitated tumor specific immunoresponses because of the presence of highly expressed tumor antigens. In addition, the DC derived immunomodulatory molecules in FMs both enhanced the antigen presentation and supported antigen-specific T cell response. As a result, the nMOF-mediated PDT combined with FM-induced immunotherapy provided strong immune responses [74].

Although the immune response activates the CTLs to kill cancer cells, the immunosuppressive TME suppressed the activation of CTLs via many negative immune mechanisms [77, 78]. To restore the function of CTLs, several studies recently reported that the application of checkpoint blockade immunotherapy,

such as IDO inhibitor, relieved the IDO-mediated immunosuppression [79]. Moreover, the above-mentioned MOFs could be efficiently loaded with IDO inhibitors in their open channels owing to the high coloading capacity. For instance, Lin et al. constructed H₄TBC-based nMOFs and used those to encapsulate IDO inhibitors in their highly porous structure for inducing systemic antitumor immunity (**Figure 4A**) [75]. They showed that the H₄TBC-based nMOFs provided PDT and ICD; further combination with checkpoint blockade therapy using IDO inhibitor enhanced T cell infiltration in TME. As a result, this synergistic treatment strategies inhibited the growth of local and distant tumors.

In addition to the IDO inhibitor, antibodies (e.g., αPD-1 and αPD-L1) are another widely used immune therapeutic agents for checkpoint blockade strategies.

For example, Zhang et al. developed benzoporphyrin-based nMOFs consisting of a Zr₆ cluster and PS (TBP) in combination with αPD-1 to inhibit tumor metastasis (**Figure 4B-E**) [76]. The benzoporphyrin-based nMOFs showed an enhanced ¹O₂ generation because of their π-extended TBP-based linkers, thus producing O₂-dependent PDT even under hypoxic tumor condition [76]. Moreover, the TBP effectively avoided ACQ because of its good dispersion in the structure of nMOFs, further facilitating PDT. Based on these advantages, the TBP-mediated PDT induced a strong ICD to recruit tumor infiltrating CTLs [76]. More importantly, the combined application of αPD-1 restored the activity of CTLs suppressed in the immunosuppressive TME [76]. In another study, Lin et al. constructed a cationic nMOF (W-TBP) highly loaded with anionic CpG via electrostatic interaction

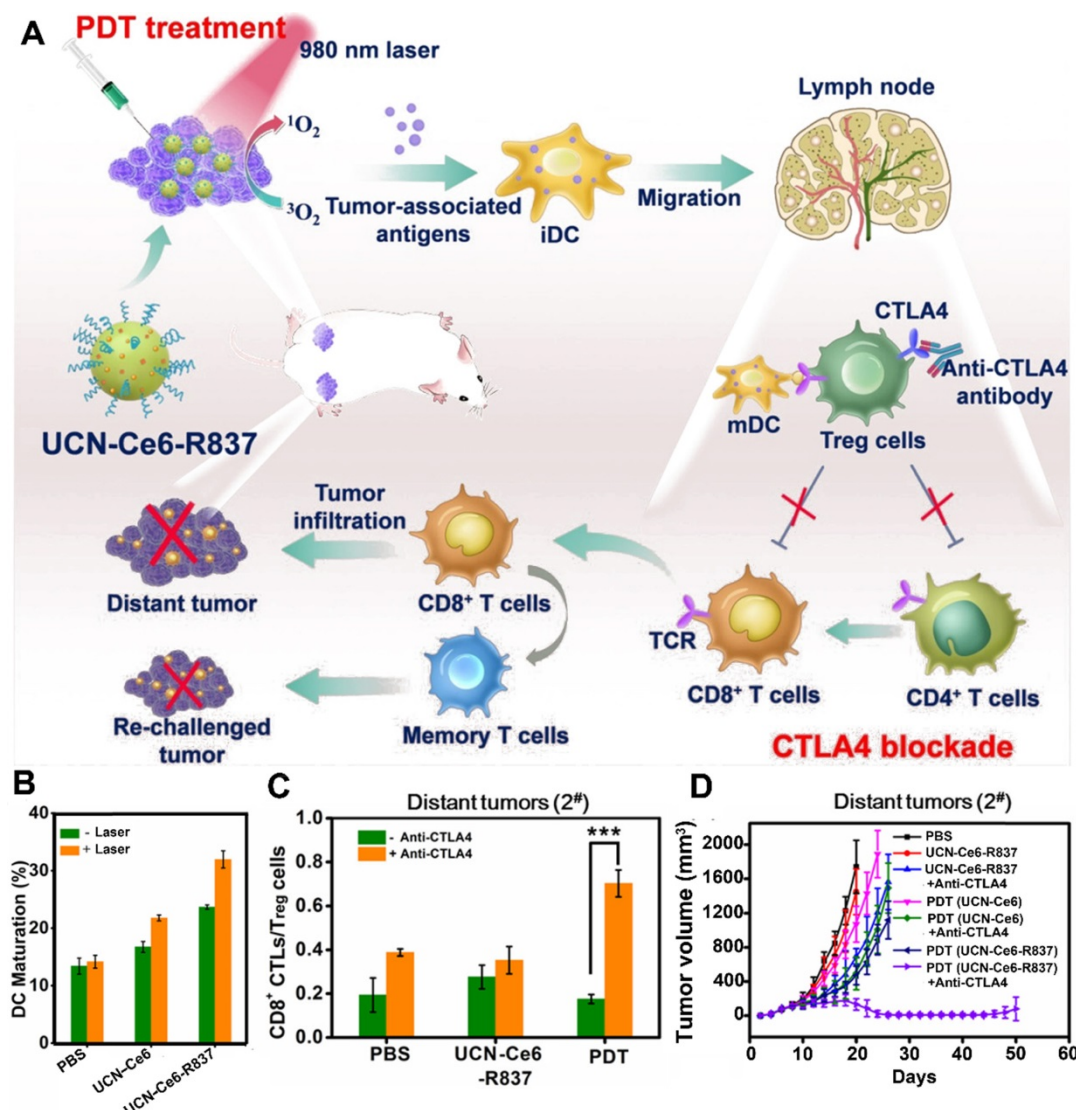


Figure 3. Upconversion NPs for PDT-driven cancer immunotherapy. (A) Schematic illustration of UCN-Ce6-R837 nanoplatform-induced strong immune response, which combined with CTLA4 blockade to inhibit the relapse and metastasis of tumors. (B) DC maturation induced by various formulations. (C) Frequency of CD8⁺ CTLs/Treg cells in distant tumors treated with different formulations. (D) Growth curves of CT26 tumor-bearing mice after receiving different formulations. Reproduced with permission [68]. Copyright 2017, American Chemical Society.

to improve cancer immunotherapy [80]. The W-TBP upon laser irradiation provided PDT, thus enhancing the release of TAAs. In addition, compared to Bi(NO₃)₃ 5H₂O-based negative nMOF, the WCl₆-based cationic nMOF showed a four-fold CpG loading capacity, which efficiently enhanced DC maturation, thereby further promoting the availability of antigen by DCs. Additionally, the αPD-1 combined with antigen availability significantly enhanced the infiltration and activation of CTLs in bilateral tumors, thus achieving a strong cancer immunotherapy [80].

2.4. TME-responsive NPs for PDT-driven cancer immunotherapy

Compared with normal tissues, solid tumors exhibit some characteristics of TME, including a low pH, severe hypoxia, and a high level of glutathione

(GSH). Hence, the development of smart stimulus-responsive nanomedicines containing TME-sensitive chemical linkers or elements can regulate the release of their cargos. In addition to advanced nMOFs, the TME-responsive NPs can also effectively avoid the ACQ by cleaving the TME-responsive linkers to rapidly release PSs at the tumor site, thus significantly improving the yield of ROS [81]. Meanwhile, the increased ROS will promote the ICD effect, thereby enhancing the immune response. Moreover, the TME-responsive NPs smartly program the location and pharmacokinetics of both PSs and immunomodulators to improve the tumor-targeting capability, leading to an enhanced PDT-driven cancer immunotherapy without causing severe side effects (Table 2).

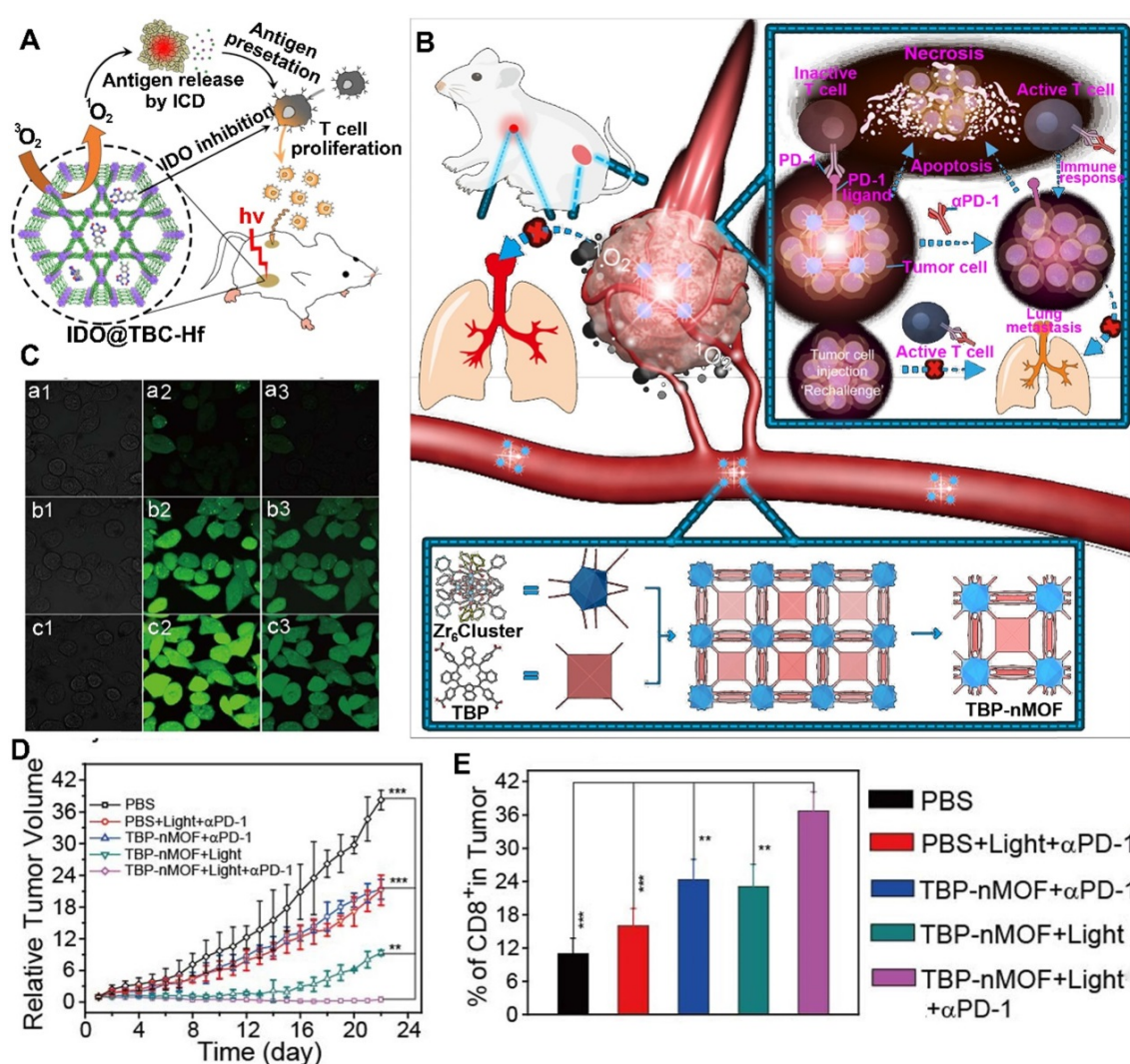


Figure 4. nMOFs for PDT-mediated Cancer Immunotherapy. Mechanism of the nMOFs to induce a PDT-mediated immune response, and combination with (A) IDO inhibitor or (B) αPD-1 in cancer immunotherapy. (C) CLSM imaging of tumor cells incubated with DCFH-DA and TBP-nMOFs in (b) under dark, (c) 5% O₂ or (d) 21% O₂ under light irradiation. (D) Growth curves of 4T1 tumor-bearing mice after receiving different formulations. (E) Frequency of CD8⁺ cells in tumors treated with different formulations. Reproduced with permission [75, 76]. Copyright 2016 and 2018, American Chemical Society.

2.4.1. pH-responsive NPs for PDT-driven cancer immunotherapy

So far, pH-responsive NPs are very common; compared to the physiological pH of 7.4 in the blood and normal tissues, more acidic environments have been found in tumors [85]. Wang et al. developed an acid-activatable multifunctional nanoplatform for PDT-mediated cancer immunotherapy [86]. This nanoplatform is composed of pH-sensitive diblock copolymer (PDPA), pheophorbide A (PPa) which is conjugated to PDPA, and PD-1-PD-L1 interaction inhibitor (siRNA). The modified diblock copolymer (termed as PDPA-PPa) was self-assembled into micelles, and the apparent pKa of PDPA is about 6.3 [86]. As the PPa was compressed into a tight hydrophobic core, this nanoplatform during blood circulation decreased the phototoxicity due to the ACQ effect. After the nanoplatform was delivered to the weakly acidified TME, the rapid dissociation of micelles caused by PDPA's "proton sponge effect" restored the photoactivity of PPa. Afterwards, the activated PPa upon irradiation generated ROS by PDT and then stimulated the expression of NF- κ B and HSP70 to provide immune response [86]. Compared to PDT alone, PDT-induced immune response combined with blocking PD-L1 pathway by using siRNA significantly enhanced the proliferation of lymphocytes and cytokine secretion, leading to a long-lasting immune response. As a result, lung metastasis was suppressed by the immune memory response [86]. Another work, Yang et al. designed pH-responsive nanovesicles (pRNVs) and coencapsulated PSs (HPPH) and IDO inhibitor (indoximod) for photodynamic immunotherapy, in which the polyethylene glycol-b-cationic polypeptide was self-assembled into pRNVs (**Figure 5A**) [36]. Compared with the pRNVs encapsulated with HPPH and IND (pRNVs/HPPH/IND) in pH 7.4 after 24 h incubation, the pRNVs/HPPH/IND in pH 5.0 showed a triple drug release rate owing to the smart nanocarriers with an excellent swelling capacity in acidic condition. Thus, the specific release of HPPH upon irradiation not only produced singlet oxygen to directly kill tumor cells by PDT, but also provided an immune response by ICD effect [87]. Surprisingly, the pRNVs also induced ICD to further improve the host immunity. More importantly, the simultaneously released IND, an IDO blockade, relieved tumor immunosuppression by restoring the mTOR pathway, thus enhancing the proliferation of CTLs [87].

2.4.2. GSH-responsive NPs for PDT-driven cancer immunotherapy

Redox potential is another possible internal stimulus for responsive release, because the concentration of GSH inside cells is almost three orders of magnitude higher than that in the extracellular plasma. Moreover, the GSH level in tumor tissues is four-fold higher than that in normal tissues [88]. Wang et al. developed a redox-activated liposome self-assembled by a porphyrin-phospholipid conjugate to synergistically work with IDO inhibitor to produce tumor immune response and reverse tumor immunosuppression (**Figure 5B**) [82]. The authors found that the porphyrin-phospholipid conjugate induced ICD by PDT after a high concentration of tumor intracellular GSH triggered the cleavage of redox-sensitive linker, while the redox-activated liposome remained silent for the photoactivity during the blood circulation period [89]. However, the ICD caused by PDT was significantly limited owing to the immunosuppressive IDO pathway. To solve this problem, IDO inhibitor (NLG-8189) was coencapsulated in a redox-activated liposome [90, 91]. It could be released by triggering the disulfide bond cleavage in tumor site to reverse the immunosuppressive TME [92]. As a result, this combination therapy of PDT-induced immunotherapy with IDO inhibitor not only suppressed the primary and abscopal tumors, but also inhibited the metastasis of breast cancer.

To avoid the leakage of encapsulated IDO inhibitor in blood circulation, Hu et al. designed a reduction-labile heterodimer of IDO inhibitor (NLG919) and PPa to achieve controllable drug release [93]. Moreover, the GSH-triggered heterodimer can integrate HA through host-guest interactions to self-assemble into supramolecular nanocomplexes. As a result, the supramolecular nanocomplexes showed excellent HA-mediated tumor targeting by recognizing CD44 overexpressed on the surface of tumor cell membranes. In addition, the biodegradability and bioactivity of HA make it a promising natural biomaterial in nanocarriers for PDT [93]. After laser irradiation, the activation of PPa generates ROS and produces antitumor immunogenicity, leading to the infiltration of CTLs into tumor site. More importantly, a combination of PDT-driven immune response and IDO-1 blockade significantly improved the antitumor efficiency compared to PDT treatment alone [93].

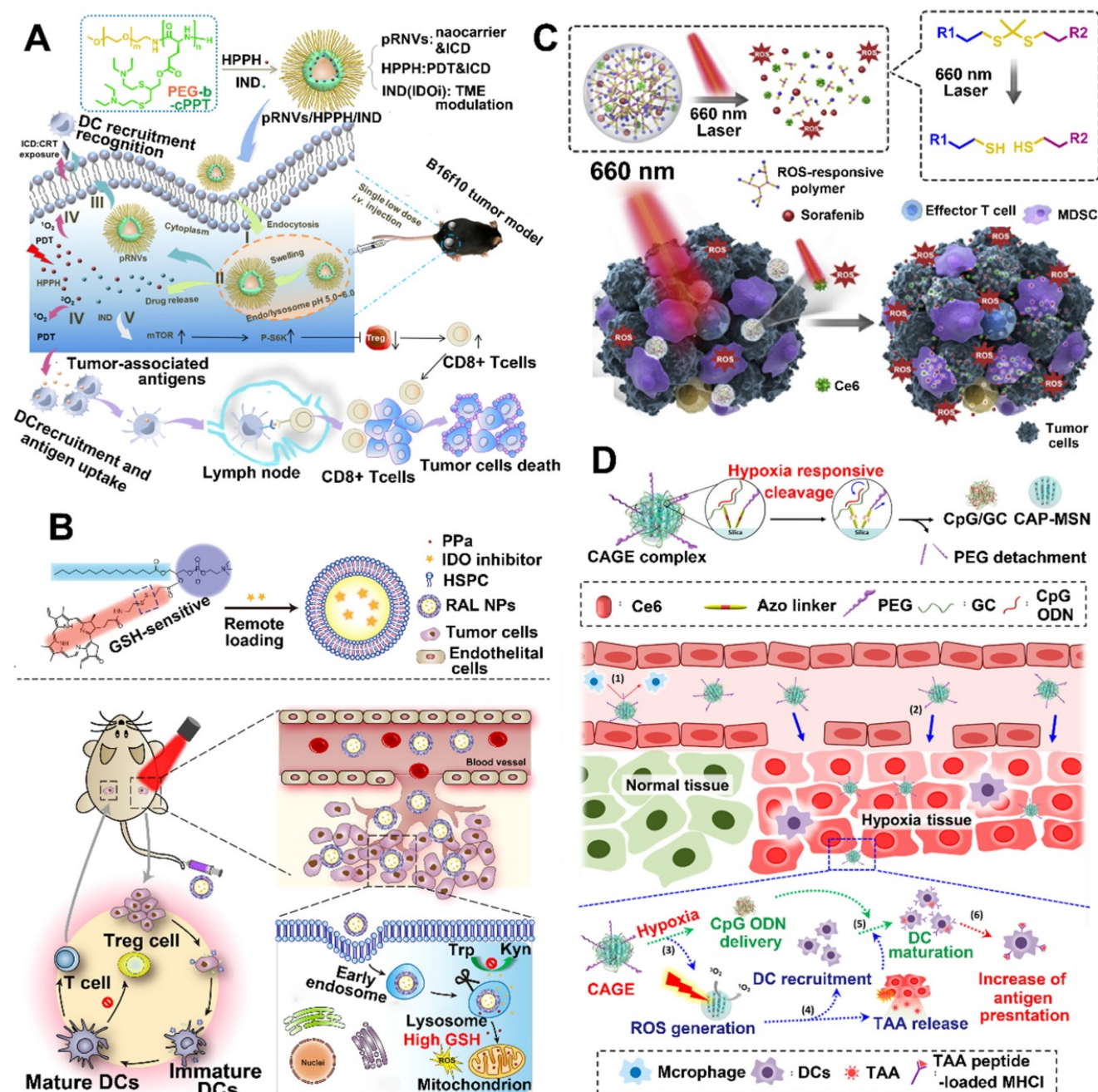


Figure 5. TME-responsive NPs for PDT-driven cancer immunotherapy. (A) Schematic illustration of pH-responsive NPs for high efficient PDT, induction of ICD, and inhibition of IDO pathway. Reproduced with permission [36]. Copyright 2020, American Chemical Society. (B) Schematic illustration of GSH-responsive NPs for PDT-induced immune response and improved tumor-targeting cancer immunotherapy. Reproduced with permission [82]. Copyright 2019, American Chemical Society. (C) Schematic illustration of ROS-responsive NPs for cascaded amplification of PDT and strong systemic antitumor immune responses. Reproduced with permission [83]. Copyright 2020, Elsevier Ltd. (D) Schematic illustration of Hypoxia-responsive NPs for hypoxia-triggered conversion, PDT-induced immune response and vaccine immunotherapy. Reproduced with permission [84]. Copyright 2019, American Chemical Society.

Table 2. Summary of emerging TME-responsive nanomedicines for PDT-driven cancer immunotherapy. (\uparrow = upregulation, \downarrow = downregulation).

Formulation	Therapeutic agents	Stimuli	Immunologic modulation	Ref
PDPA-PPa micelles	PPa, SiRNA	pH	TAAs, mDC, HSP70, CD8 \uparrow , NF- κ B \uparrow PD-L1 \downarrow	86
pRNVs/HPPH/IND nanovesicles	HPPH, pRNVs, IND	pH	TAAs, DC, mTOR, CD8 \uparrow Treg \downarrow	36
porphyrin-phospholipid liposomes	PPa, NLG-8189	GSH	TAAs, mDC, CD8 \uparrow , INF- γ , Trp \uparrow Kyn \downarrow	82
supramolecular nanocomplexes	PPa, NLG919	GSH	TAAs, mDC, CD8 \uparrow , Trp \uparrow Treg, Kyn \downarrow	93
biodegradable inorganic NPs	Ce6, CpG	GSH	TAAs, mDC, CD8 \uparrow	96
NP-sfb/Ce6 NPs	Ce6, sorafenib	ROS	TAAs, mDC, CD8 \uparrow MDSCs \downarrow	83
Ce6-doped mesoporous silica NPs	Ce6, CpG	Hypoxia	TAAs, mDC, CD4 \uparrow , CD8 \uparrow	84
hypoxia-activatable polymeric micelles	DOX, ICG, CpG, α CTLA4	Hypoxia	TAAs, mDC, CD4 \uparrow , CD8 \uparrow TNF- α , IFN- γ , IL-12p70 \uparrow	104
Boolean logic prodrug NPs	PPa, NLG919	pH/GSH/MMP-2	TAAs, mDC, CTLs, Trp \uparrow Treg, Kyn \downarrow	108

In addition to organic nanocarriers, inorganic nanocarriers (e.g., mesoporous silica NPs (MSNs)) are also an important branch to deliver PSs for PDT, as they have many advantages, including tunable size, prone to surface modification, and high colloidal stability [94]. Because inorganic nanocarriers are difficult to degrade and easily cause accumulation toxicity, their application is limited [95]. Recently, many studies have been devoted to the development of biodegradable inorganic NPs by introducing sensitive bonds; thus, the abovementioned problem has been significantly improved. For example, Xu et al. constructed a GSH-responsive biodegradable multifunctional nanosystem for personalized cancer immunotherapy against local and metastatic tumors [96]. The obtained multifunctional nanosystem consisted of MSNs conjugated with neoantigen peptides via disulfide bond [96], in which Ce6 and CpG oligodeoxynucleotide adjuvant were coencapsulated. Upon PET imaging, the multifunctional nanosystem after intravenous administration was effectively accumulated in tumors. Meanwhile, the accumulated Ce6 initiated PDT after laser irradiation, and then PDT-treated tumor sites would recruit numerous DCs to induce ICD [96]. Furthermore, the GSH-triggered release of personal neoantigen increased the antigen availability by DCs, which is also a requisite factor for inducing ICD. Therefore, PDT combined with personal neoantigen plus CpG adjuvants achieved synergy, thereby further enhancing the ICD and realizing neoantigen-specific immune response [96].

2.4.3. ROS-Responsive NPs for PDT-driven cancer Immunotherapy

The encapsulation within or conjugation to a ROS-responsive nanocarrier can regulate the release of PSs because tumor cells with higher ROS levels initiate the cleavage of sensitive bonds [97, 98]. In addition, the released PSs stimulated by laser irradiation can also produce exogenous ROS. Therefore, the PS-generated ROS combined with intracellular ROS can provide a cascading amplification effect to remotely control the release of cargos [99]. For instance, Su et al. designed a multifunctional nanoplatform (NP-sfb/ce6) by encapsulating Ce6 and sorafenib in ROS-responsive polymeric NPs for antitumor immunotherapy (**Figure 5C**) [83]. First, they synthesized PEGylated hyperbranched polyphosphates with ROS-responsive capability by inserting thioketal linkers and used them to construct polymeric NPs [83]. After laser irradiation, the NP-sfb/ce6 was rapidly disassembled because the PDT-generated singlet oxygen cleaved the thioketal linkers, leading to a cascade amplification to

enhance the drug release of sorafenib. In addition, low-dose PDT significantly inhibited the primary tumor growth as well as distant tumor growth by combining with the rapidly released sorafenib, due to synergistically inducing ICD, reversing the immunosuppressive TME and increasing the infiltration of CTLs [83].

2.4.4. Hypoxia -responsive NPs for PDT-driven cancer immunotherapy

Unlike the abovementioned strategies to ameliorate hypoxia TME, application of tumor hypoxia by rapidly transforming large-sized NPs to small-sized nanocomplexes would better regulate the delivery of nanocarriers *in vivo* and accumulation of tumor sites [100, 101]. This is because the large sized NPs will undergo long blood circulation, while the small sized NPs can achieve deep tumor penetration or accumulation in specific organs, such as lymph nodes and kidney [102]. Recently, a big challenge still exists for cancer vaccines that improve the delivery efficiency of both neoantigens phagocytized by DCs and adjuvant to tumor draining lymph nodes (DLNs) [84]. To solve this problem, Kim et al. prepared a Ce6-doped mesoporous silica nanocarrier decorated with a PEGylated azobenzene linker, which was loaded with CpG and glycol chitosan (GC), in which the CpG and GC could form complexes through electrostatic interaction (**Figure 5D**) [84]. Once this nanoplateform arrives at a hypoxia TME, the hypoxia-responsive bond (azobenzene linker) will be rapidly cleaved to release the CpG/GC complex. Furthermore, the Ce-6 generated ROS upon laser irradiation not only induced PDT but also enhanced the cleavage of azobenzene linker due to further oxygen consumption by PDT [84]. Moreover, the tumor cells after treating with PDT produced neoantigens and subsequently phagocytized by DCs to provide immune response. In addition, they showed that PEGylated NPs successfully escaped from DLNs to accumulate at the tumor site, while dePEGylated NPs reached the DLNs by cleaving the hypoxia-responsive labile linker and then endocytosed by DCs, thereby improving the antigen presentation activity of DCs [84, 103]. In another study, Mi et al. designed hypoxia-activatable polymeric micelles to skillfully integrate therapeutic agents into one nanosystem. After arriving at the hypoxia tumor tissue, the nanosystem was selectively activated to release the therapeutic agents. Subsequently, the released agents not only eradicated the primary tumors, but also induced robust systemic immune responses. More importantly, this nanosystem in combination with CpG and aCTLA4 achieved a synergistic effect to inhibit tumor

metastasis and recurrence [104].

2.4.5. Multiple-responsive NPs for PDT-driven cancer immunotherapy

In biological systems, the change in the behavior of a biomacromolecule is often a result of its response to a combination of multiple environmental changes [105]. To further improve the tumor-targeted drug delivery, Boolean logic operations involving logic-gated devices have drawn increasingly more attention. Based on Boolean logic rules, better logic operations were established by incorporating more input signals (e.g., tumor hallmarks) [106, 107]. Inspired by this feature, construction of versatile nanoplatforms which can respond to multiple stimuli of pH/GSH/enzyme would facilitate the on-demand release of therapeutic cargos. For example, Hou et al. designed Boolean logic prodrug NPs (BLPNs) for precise cancer immunotherapy [108]. The BLPNs are composed of two biologically stimulant-responsive polymer prodrugs, one of which is conjugated with an immune activator (PPa) and the other is modified to an immune inhibitor (NLG919) by disulfide bond. In addition, both the polymer prodrugs were PEGylated by inserting MMP-2/9-responsive peptide and showed an ultra-pH-sensitive capability because of the presence of the structure of 2-(diisopropylamino)ethyl methacrylate. Based on Boolean logic, a series of BLPNs obtained by adjusting the input combinations of three tumor hallmarks (pH/GSH/enzyme) will yield different YES/AND logic outputs. They found that the BLPNs improved the deep tumor penetration and cellular uptake by MMP-2-mediated dePEGylation. With the progress of the protonation in the endosomal vesicles of cancer cells, the BLPNs would rapidly dissociate to acquire acid-activatable photoactivity, and then produce PDT-induced immune response upon laser irradiation. More importantly, the GSH-triggered drug release of NLG919 controllably reversed the immuno-suppressive TME by inhibiting the IDO pathway. As a result, this multiple-responsive nanoplatform achieved precise cancer immunotherapy by using Boolean logic operations [108].

2.5. Subcellular targeted NPs for PDT-driven cancer immunotherapy

So far, several smart nanotechnology formulations have been developed to deliver PSs into tumor tissue by utilizing the EPR effect. Upon a local laser irradiation, the PS-generated ROS damage adjacent biomolecules, thereby inducing PDT [109, 110]. However, ROS (e.g., ${}^1\text{O}_2$) has a short lifespan, significantly limiting their diffusion in cytoplasm as well as among tumor cells, causing a discounted PDT

efficacy [111, 112]. Therefore, precise delivery of PSs to ROS-related subcellular organelles (including ER [113], mitochondrial [114], lysosome [115], and cell nucleus [116]) as well as plasma membrane (PM) [117] effectively avoided the fast decay of cytoplasm-localized PDT (cPDT)-derived ROS, leading to a maximal antitumor effect of PDT.

ER in the cell plays a role in the synthesis and transport of protein, intracellular calcium storage, and the regulation of intracellular calcium levels to maintain its balance. Cell apoptosis mediated by ER pathway has become a new field of research on apoptosis [121]. As mentioned above, ROS-mediated PDT induced ICD by causing sequential changes including, but not limited to, CRT exposure and HMGB1 release to produce immune response [34, 122]. Recently, several studies showed that the CRT is located in ER, so that the ROS-induced ER stress provided a high-efficiency boost to CRT exposure to evoke a strong ICD [123-125]. For example, Deng et al. synthesized a ER-targeted PS (TCPP-T^{ER}) using *N*-tosylethylenediamine as the PS (TCPP) and a reduction-sensitive polymeric conjugate (Ds-sP) (**Figure 6A**) [118]. Subsequently, the synthesized Ds-sPs simply self-assembled into NPs, with TCPP-T^{ER} coencapsulated into the nanostructures. In the presence of GSH, the self-assembled Ds-sP/TCPP-T^{ER} was rapidly destabilized and enhanced the release of TCPP-T^{ER}, because GSH triggers the cleavage of reduction-sensitive linkers. Compared to TCPP-T, the released TCPP-T^{ER} from Ds-sP/TCPP-T^{ER} by using *N*-tosylethylenediamine showed an excellent ER targeting capability and *in situ* ROS generation, leading to an enhanced ER stress [118]. Furthermore, they found that Ds-sP/TCPP-T^{ER} under laser irradiation induced more CRT exposure on the membrane of tumor cells in comparison with Ds-sP/TCPP-T, providing amplified ICD, thus resulting in the enhanced infiltration of CTLs.

In addition to ER, another ROS-sensitive subcellular organelle, mitochondria, has drawn much attention in increasing the efficiency of PDT [126-128]. As the cells' powerhouse, the mitochondria are tightly linked to many intracellular activities, including programmed cell death (apoptosis), ROS generation, and ATP production [129, 130]. Furthermore, cell apoptosis and release of ATP are associated with ICD. Therefore, delivery of PSs to mitochondria using a reasonable nanosystem could be a potential strategy for enhancing cancer immunotherapy [87, 119]. For example, Liu et al. designed mitochondria-targeting NPs loaded with Ce6 to improve PDT-mediated immunotherapy, in which a triphenylphosphonium (TPP)-modified cationic hollow silica precursor acted as nanocarriers (**Figure 6B**) [87]. Subsequently, the

positively charged core coated with a negatively charged pH-responsive PEG layer by electrostatic interaction acted as a protective shell [87]. Thanks to the negatively charged pH-responsive PEG layer, the mitochondria-targeting micelles with a positive charge avoided rapid clearance during the circulation, thus leading to an obvious tumor accumulation. After reaching the acidic TME, the pH-responsive PEG layer was rapidly decomposed and exposed the TPP molecules, thus increasing the cellular uptake of positively charged micelles and recovering the targetability to the mitochondria. More importantly, the Ce6-loaded micelles upon laser irradiation induced improved immune responses via ROS generation in mitochondria [87, 119].

Compared with conventional cPDT-induced apoptosis, necrosis provides a more immunogenic result from the accelerated release of DAMPs [131, 132]. PM-targeted PDT led to PM rupture by causing a

series of changes (e.g., enhanced membrane permeability and lipid peroxidation) [133]. Subsequently, PM rupture induced cell necrosis by rapidly releasing the intracellular contents, thus leading to a strong antitumor immune response [120]. For instance, Zhang et al. constructed enzyme-driven PM-targeted NPs (PCPK NPs) self-assembled from chimeric peptide (PpIX-C₆-PEG₈-KKKKKKSKTKC-OMe, termed as PCPK) (Figure 6C) [120]. The self-assembled PCPK NPs acquired the PM targeting ability through the protein farnesyltransferase (PFTase)-mediated enzymatic conversion, and then the obtained farnesylated product was tightly anchored on the PM [134-136]. After laser irradiation, the PCPK produced PM-localized ROS and subsequently induced an intense PDT efficacy, resulting in lipid peroxidation and PM rupture. This localized PDT-driven PM damage induced an obvious cell necrosis to rapidly release ATP and HMGB1,

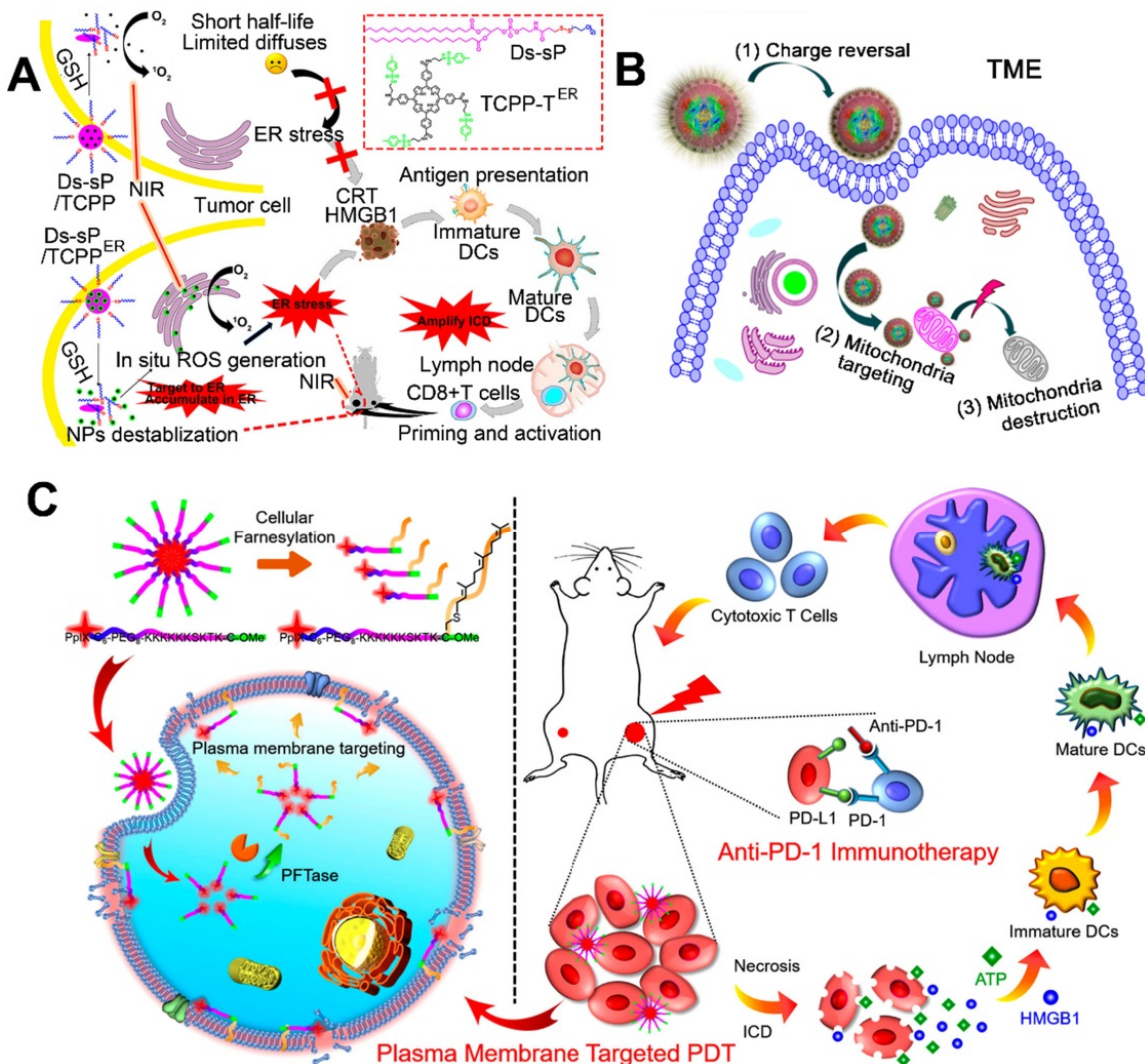


Figure 6. Schematic illustration of various subcellular targeted NPs for improved PDT-driven cancer immunotherapy. (A) ER-targeting Ds-sP/TCPP-T^{ER} NPs, (B) Ce6-loaded mitochondrial-targeting NPs, (C) enzyme-driven PM-targeting PCPK NPs. Reproduced with permission [118, 87, 120]. Copyright 2020, American Chemical Society; Copyright 2018, American Chemical Society; Copyright 2019, American Chemical Society.

leading to a strong immune response [120]. More importantly, this PM-PDT strategy in combination with checkpoint blockade therapy effectively inhibited the growth of metastatic tumor.

2.6. Carrier-free and small-molecule prodrug-based self-assembled NPs for PDT-driven cancer immunotherapy

Different from multifunctional polymeric nanocarriers requiring complex preparation technologies and potential toxic excipients, carrier-free nanoplates could be self-assembled from pure therapeutic drugs for delivering PSs without causing side effects from using additional excipients [137, 138]. For instance, Wang et al. constructed a TME-activatable carrier-free nanoplate composed of ICG and αPD-L1 for combination immunotherapy (**Figure 7A**) [139]. They showed that the ICG and αPD-L1 could be simply self-assembled into NPs via electrostatic interactions and hydrophobic force, exhibiting a diameter of approximately 14.5 nm in size. Moreover, the self-assembled NPs modified with the MMP-2-labile PEG corona (carrier-free nanoplate) led to a prolonged blood circulation and thus prevented the compressed αPD-L1 from interacting with normal organs [139]. In addition, the carrier-free nanoplate could be selectively triggered to release ICG and αPD-L1 by utilizing the tumor overexpressed MMP-2, thereby significantly enhancing the accuracy of αPD-L1-based checkpoint blockade therapy. More importantly, the controllable release of ICG produced local ROS to induce strong immune response, which further cooperates with αPD-L1 to achieve high-efficiency cancer immunotherapy for inhibiting tumor growth and metastasis [139]. To improve the accuracy of image-guided PDT, Xu et al. designed multifunctional nanocomplexes for a combination delivery of Ce6 and immunoglobulin G (e.g., αCTLA-4 and αPD-L1) [140]. The authors revealed that the Ce6 showed a higher affinity to immunoglobulin G compared with previous reported HSA. Furthermore, immunoglobulin G and Ce6 could be self-assembled into stable NPs (chloroglobulin) with the addition of polyvinylpyrrolidone, significantly improving the intratumoral concentration of Ce6 without affecting its metabolic rate in blood [140]. Compared with the traditional strategies to deliver PSs, this “immunoglobulin G hitchhiking” approach improved the tumor accumulation of Ce6 and then induced strong immune response to confront the limited clinical treatment effect of checkpoint blockade therapy due to low tumor immunogenicity [140]. Therefore, the αPD-L1-based chloroglobulin

achieved a cooperative therapy by the integration of PD-L1 blockade therapy, Ce6-mediated PDT, and fluorescence image-guided surgery. More importantly, the authors showed that the dual checkpoint blockade (αCTLA-4 and αPD-L1) therapy in combination with the PDT-induced ICD further enhanced the cancer immunotherapy [140, 141].

Besides the carrier-free self-assembled NPs, the small-molecule prodrug-based self-assembled NPs also have a great potential in clinical translation for anticancer therapy owing to their high drug delivery ability and avoidance of using toxic excipients [142]. For example, Zhang et al. constructed a novel small-molecule prodrug (PpIX-1MT) by conjugating the checkpoint inhibitor (1 MT) to PS PpIX by inserting a caspase-responsive chimeric peptide, and then the synthetic PpIX-1MT was self-assembled into NPs (**Figure 7B**) [90]. After reaching the tumor site, the PpIX-1MT NPs under laser irradiation generated ${}^1\text{O}_2$ to cause cancer cell apoptosis, which further activated the overexpression of caspase-3 [90]. The overexpressed caspase-3 in turn rapidly cleaved the caspase-responsive linker to enhance the release of PpIX and 1MT. The released PpIX enhanced the production of ${}^1\text{O}_2$ to induce a strong immune response, and the synchronously released 1-MT achieved a cascaded synergistic effect in cancer immunotherapy by relieving the immunosuppressive TME [90].

3. Emerging nanomedicines for multi-factor-driven cancer immunotherapy

Although PDT can induce immune response by ICD in certain tumors, its effect is significantly hindered by the complex immunosuppressive TME [143]. Therefore, monotherapy based on PDT usually exhibits a limited efficacy to induce antitumor immunity. Recently, several therapeutic strategies also can initiate ICD by directly killing tumor cells, including radiotherapy, chemotherapy, and photothermal therapy (PTT) [34, 35]. Combination of multiple therapies might achieve a synergistic effect to increase the intensity of immune response. Nanomedicine-based delivery can coencapsulate different drugs into one nanoplate and alleviate the side effect due to nonspecific systemic distribution. We discuss emerging nanomedicines for improving the immune response by combination strategies such as PDT/ chemotherapy and PDT/PTT. More importantly, the combination strategies plus checkpoint blockade immunotherapy will achieve a durable and efficient antitumor treatment effect.

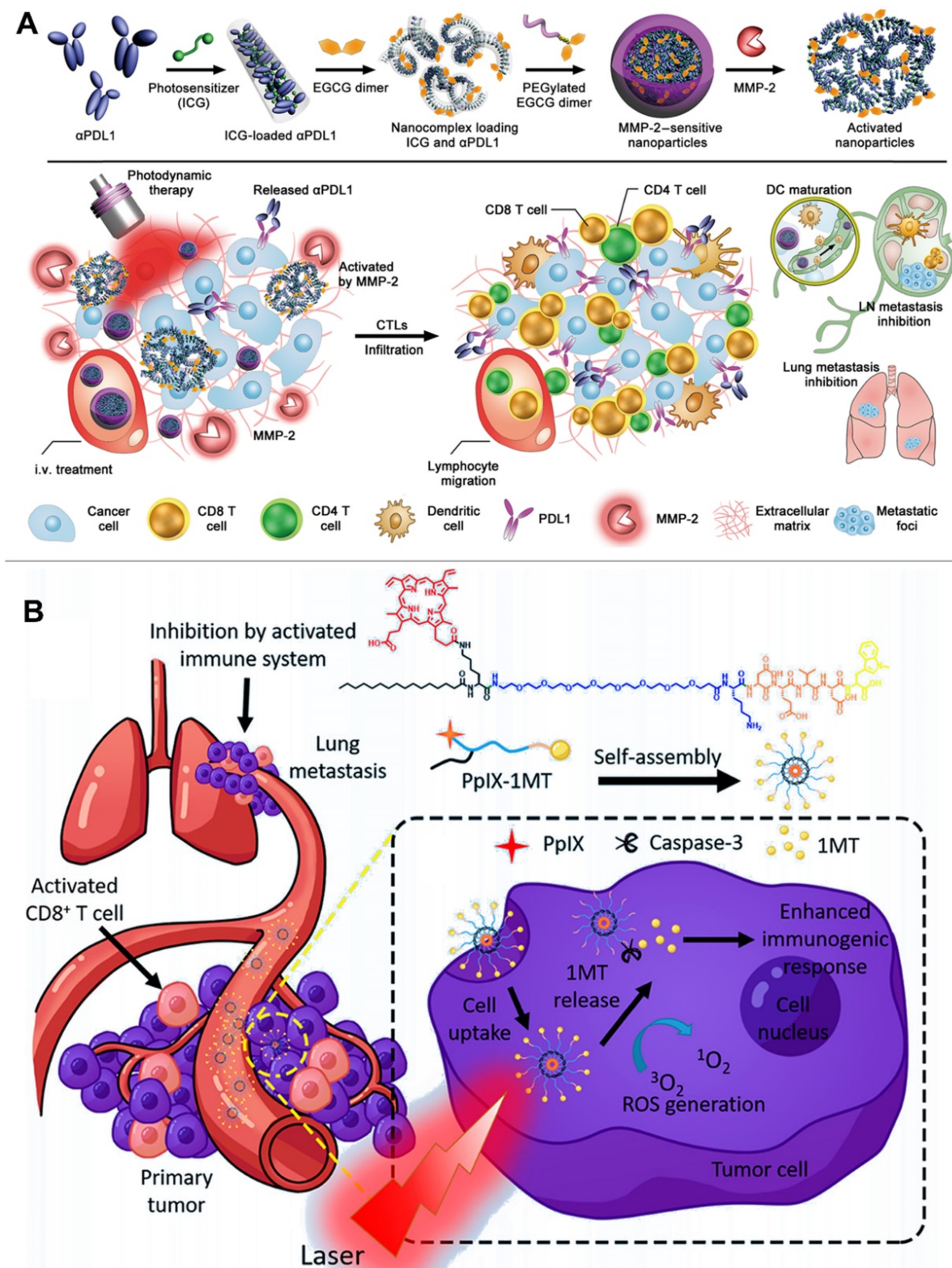


Figure 7. (A) Schematic illustration of preparation of the PEG-coated co-assembled NPs of ICG and α PD-L1, *in vivo* local activation of cancer immunotherapy. Reproduced with permission [139]. Copyright 2019, AAAS. (B) Schematic illustration of preparation of small molecule prodrug self-assembled NPs for *in situ* PDT, increased immunogenic response, cascade release of IDO inhibitor, inhibition of lung metastasis. Reproduced with permission [90]. Copyright 2018, American Chemical Society.

3.1. Emerging nanomedicines for PDT-chemo-driven cancer immunotherapy

For a long time, chemotherapy has been the

mainstay of cancer treatment. Hence, chemotherapy combined with other therapies always draw much more attention [18]. Some chemotherapeutic agents (e.g., doxorubicin) can trigger ICD to induce systemic

immune response [34]. Chemotherapy-mediated ICD facilitates the release of danger signals (e.g., CRT) from dying tumor cells, which is similar to PDT-mediated ICD, and then achieve a synergistic effect to enhance immune activation [18]. For example, Chen et al. developed chimeric cross-linked nanovesicles (CCNVs) self-assembled from a triblock copolymer, which both acted as nanocarriers and adjuvants (**Figure 8**) [144]. With the conjugation of protonatable groups, the CCNVs simply escaped from the endosome after cellular internalization. In addition, the cross-linked structure via thiol groups not only helped to avoid drug leakage, but also regulated the release of loaded cargos in response to GSH. After the coencapsulation of HPPH and DOX, the CCNV/DOX/HPPH under laser irradiation induced ICD by both DOX and HPPH-mediated PDT, which would achieve a combinational effect to improve DC recruitment and TAA secretion in tumor site [144]. Furthermore, the embedded amines of CCNV effectively enhanced antigen presentation and DC maturation by acting as an adjuvant. As a result, this smart *in situ* DC vaccine strategy induces an intense immune response by the integration of chemotherapy, PDT, and immunotherapy [144]. Furthermore, Yang et al. designed cascade chemo-PDT by using a ROS-responsive nanoplatform (^{TK}HNP-C/D) composed of a polymer-lipid hybrid nanocarrier as well as the coencapsulation of DOX and Ce6 to provide the checkpoint blockade immunotherapy [145]. In their study, the hybrid nanocarrier consisted of a hydrophilic shell and a hydrophobic core: The hydrophilic shell includes DSPE-PEG and neutral lipid lecithin to increase the stability and drug loading efficiency of nanocarriers; the hydrophobic core contains a ROS-responsive poly(thioketal phosphoester) to regulate the release of loaded cargos [145]. They found that the ^{TK}HNP-C/D upon laser irradiation cleaved the ROS-sensitive groups by the Ce6-generated ROS and in turn accelerated the release of Ce6 and DOX, leading to a self-amplified ROS-induced PDT. In addition, the released DOX combined with the Ce6-generated ROS achieved a cascade chemo-PDT to trigger a strong antitumor immune response by facilitating DC recruitment and CTL infiltration to tumor site. More importantly, the αPD-L1 in combination with ^{TK}HNP-C/D plus laser irradiation generated an immune memory effect to inhibit distant tumor growth [145].

Apart from DOX, oxaliplatin (OXA) causes the release of DAMPs to effectively induce ICD, leading to a strong immunity response [146]. For example, He et al. developed a core-shell nanoplatform to improve checkpoint blockade immunotherapy, in which the

shell included pyropheophorbide-lipid conjugates (pyrolipid) to induce PDT, and the core contained oxaliplatin prodrugs to produce chemotherapy [146]. The authors found that the synthetic OXA prodrug and pyrolipid of this core-shell nanoplatform not only enhanced the drug loading capability of parent drugs (oxaliplatin and pyropheophorbide-a), but also prolonged their blood circulation [146]. Moreover, the pyrolipid-induced PDT synergized with OXA-elicited chemotherapy to promote CRT exposure and antigen presentation, resulting in tumor-specific immune responses. Furthermore, this synergized chemo-PDT plus αPD-L1 therapy effectively inhibited the metastatic metastasis of colorectal cancer. Besides the checkpoint blockade of PD-L1, the CD47 blockade has been utilized in clinical trials [147-149]. For instance, Zhou et al. constructed TME-responsive prodrug vesicles in combination with CD47 blockade for cancer immunotherapy [150]. In this study, prodrug vesicles underwent a charge transformation at tumor tissue by the MMP-2-triggered cleavage of PEG-PS conjugates, which not only enhanced the cellular uptake and deep tumor penetration, but also selectively released the PS. After internalization by tumor cells, the prodrug vesicles rapidly released OXA in response to GSH. Furthermore, the released OXA and PS plus laser irradiation reached a synergic chemo-PDT to induce ICD, and further utilized CD47 blockade to relieve immunosuppression, leading to a combinational strategy for cancer immunotherapy [150]. To further enhance the drug delivery efficacy, Feng et al. synthesized a GSH-responsive heterodimer of NLG919 and PPa, which could be simply self-assembled into NPs due to the insertion of disulfide bond, resulting in an ultrahigh drug loading [151]. To improve the stability and tumor accumulation of NPs, a thioketal bond-linked PEGylated OXA prodrug served as a protective shell. After the first wave light irradiation, the PEGylated NPs produced numerous PPa-mediated ROS, which triggered dePEGylation by the cleavage of thioketal bond, leading to deep tumor penetration. After internalization by tumor cells, the dePEGylated NPs not only facilitated the release of NLG919 and PPa via the GSH-induced degradation of heterodimer, but also increased the OXA release form prodrug. After second light irradiation, the released OXA and PPa achieved a synergistic chemo-PDT to induce immune response. Furthermore, the GSH-mediated NLG919 release suppressed IDO-1 activity to relieve immunosuppressive TME [151].

PDT itself involves continuous oxygen consumption, which would further aggravate tumor hypoxia [152-154]. Recently, studies constructed hypoxia-activated prodrug (HAP) nanoplatforms

instead of aforementioned hypoxia relief strategies to enhance anticancer treatment [155-157]. For example, Shao et al. developed tirapazamine (TPZ)-loaded UCN@MOFs (TPZ/UCSs) to achieve combinational chemo-PDT (Figure 9) [157]. With the special heterostructure, UCSs absorbed long-wavelength light (LWL), and further transferred energy from UCNs to PS, resulting in a deeper-penetrating PDT. In this study, the PS-based MOF has a high PS loading ability, and the well-dispersed PSs effectively avoided self-quenching to induce PDT [157]. Furthermore, the

loaded TPZ, a hypoxia-activated prodrug, was efficiently activated by the PDT-aggravated tumor hypoxia. Subsequently, the activated TPZ produced toxic oxidizing radical species, which further synergized with the Ce6-generated ROS to induce a strong antitumor immune response. More importantly, the integration of αPD-L1 with TPZ/UCSs produced specific tumor infiltration of CTL to suppress distant tumors through this combinational strategy of immunotherapy, hypoxia-activated chemotherapy, and LWL-mediated PDT [157].

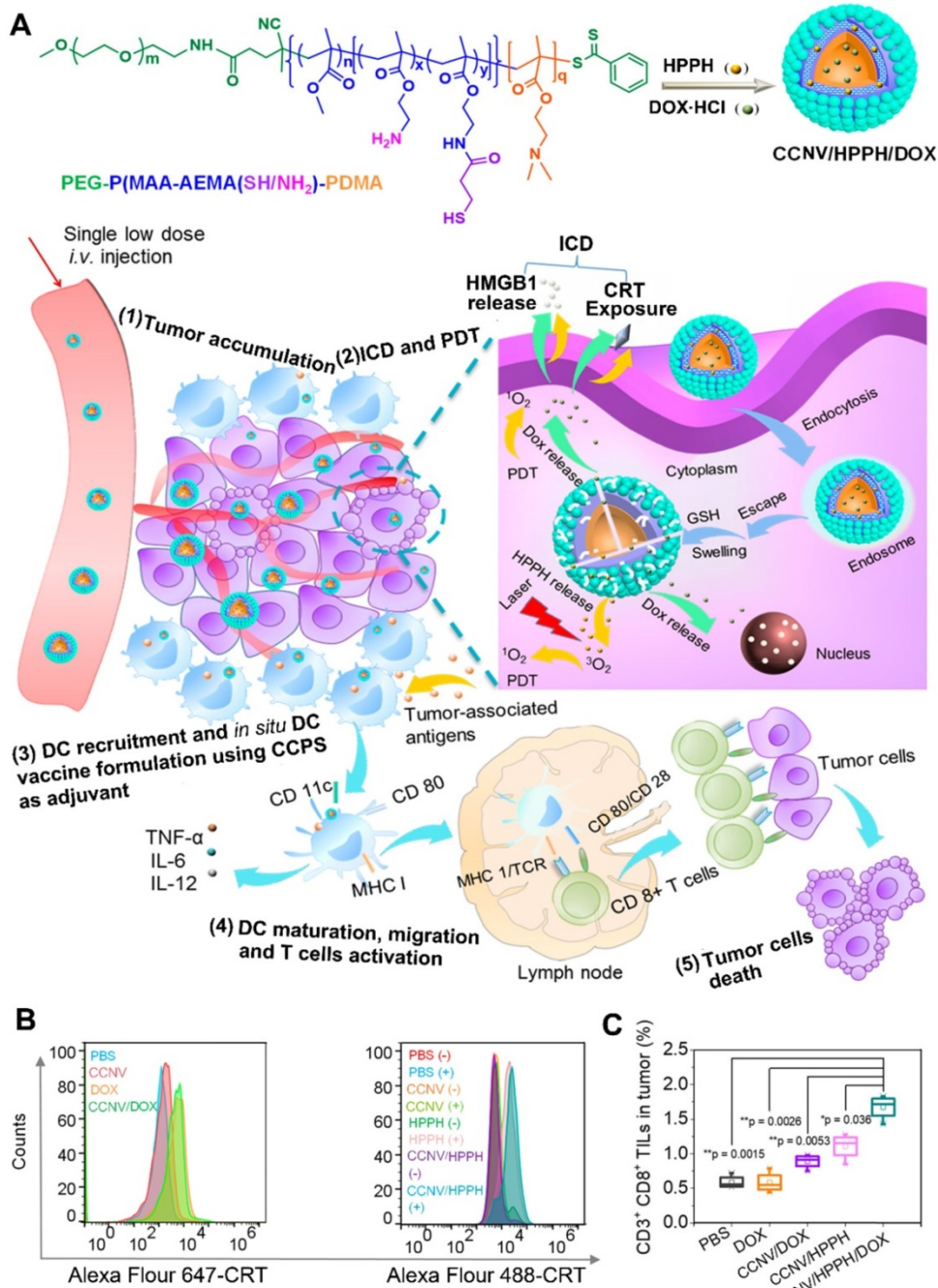


Figure 8. (A) Schematic illustration of preparation of CCNV/DOX/HPPH as *in Situ* DC Vaccine for synergistically inducing ICD by chemotherapy and PDT, CTL activation and vaccine immunotherapy. (B) Flow cytometry characterization of CRT exposure by measuring various formulations stained with specific fluorescent probe of CRT. (C) Frequency of CD3⁺ CD8⁺ TILs in tumors treated with different formulations. Reproduced with permission [144]. Copyright 2019, American Chemical Society.

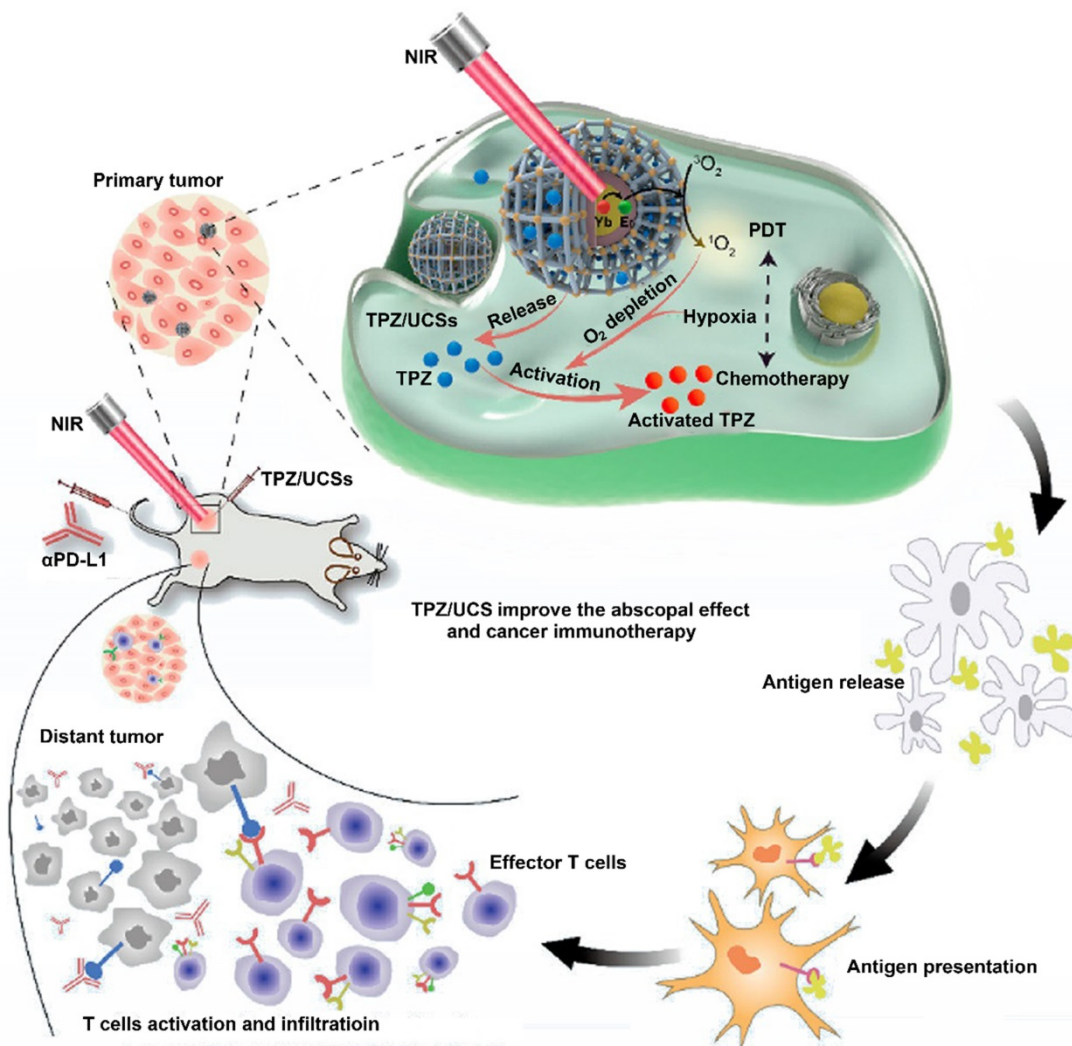


Figure 9. Schematic illustration of UCN@MOF nanostructures loaded with TPZ for cancer treatment by integration of hypoxia-activated chemotherapy, NIR light-triggered PDT and immunotherapy. Reproduced with permission [157]. Copyright 2020, American Chemical Society.

3.2. Emerging nanomedicines for PDT-PTT-driven cancer immunotherapy

Using the photo-absorbing agents, PTT achieved targeted-tissue-specific therapy via converting light into heat and synergized with the oxygen-dependent PDT against hypoxic tumor. In addition, this localized thermal ablation effect also induced ICD, leading to the desired antitumor immune responses [158-160]. So far, many photothermal agents (PTAs) have been reported, such as inorganic metals, transition metals, magnetic materials, organic dyes, organic polymers, and organic semiconductor [57, 161-165].

Inorganic PTAs have many advantages in PTT-mediated cancer treatment, including strong NIR responsiveness, resistance to photodegradation, and high photothermal conversion efficiency. Therefore, inorganic PTAs are an excellent choice to induce strong immune responses. For example, You et al. designed a dual ER-targeting nanosystem composed

of ICG-grafted hollow gold NPs (FIAuNPs) modified with pardaxin (FAL) peptides and FAL-modified O₂-carrying Hb liposomes (FHlipos) to achieve a synergistic PDT-PTT-induced immunotherapy (**Figure 10A**) [57]. Thanks to the modification of FAL peptide, this nanosystem realized ER-targeted accumulation and direct ROS-based ER stress, leading to ER-localized PDT. To relieve tumor hypoxia, the FHlipos released O₂ from Hb, further enhancing the efficiency of ER-localized PDT [57]. In addition, this FIAuNPs under laser irradiation resulted in tumor hyperthermia (PTT) due to the special structure of ICG-grafted hollow gold NPs, which effectively converted light into heat [57]. Furthermore, they showed that the integration of ER-targeting PDT-PTT caused much more CRT exposure, DC maturation, and proliferation of CTLs compared with nontargeting nanosystem, leading to a promoted ICD-associated immunological response (**Figure 10B**) [57]. To further enhance the effect of PDT and PTT,

Chang et al. modified Cu₂MoS₄ (CMS) nanosheets with the deposition of plasmonic gold NPs to develop novel CMS/Au heterostructures, which showed a widened optical absorption band based on orbital hybridization [161]. Compared to single CMS, the CMS/Au heterostructures triggered the reaction of H₂O₂ to produce O₂ by acting as catalysts and further

improved the effect of PDT by relieving tumor hypoxia. Based on these advantages, they found that PDT-PTT induced by CMS/Au heterostructures enhanced cytokine secretion and DC maturation to elicit immune responses and produce a memory effect of CTLs to suppress tumor metastasis.

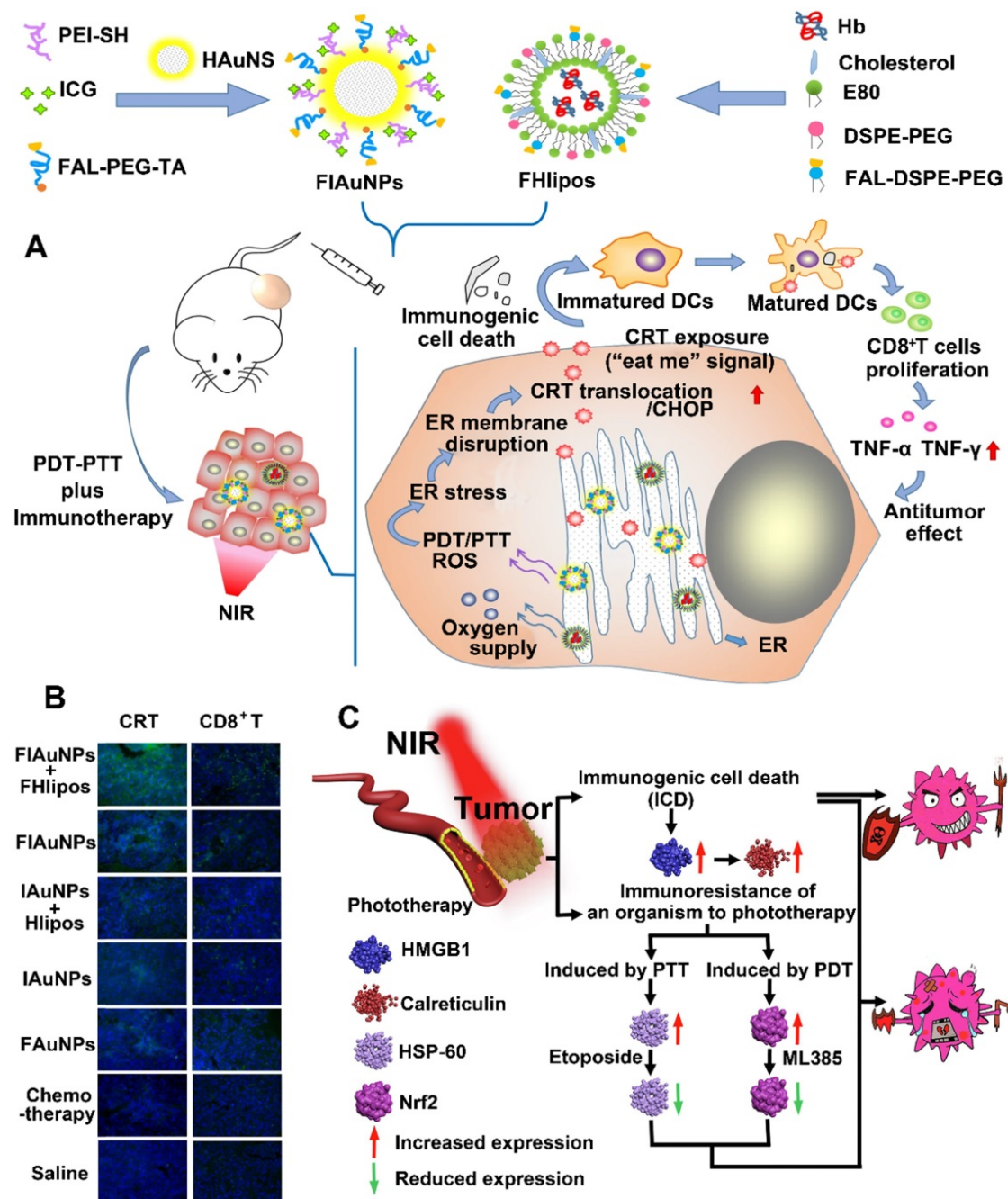


Figure 10. (A) Schematic illustration of preparation of ER-targeting and ER-targeting FIAuNPs and FHlipos for combinational therapeutic strategies including ER-targeting PTT, ER-targeting PDT, and synergistically inducing ICD by PTT and PDT. (B) CLSM imaging of tumor sections treated with various formulation for detecting immunofluorescent staining of CD8⁺ T cells and CRT expression. Reproduced with permission [57]. Copyright 2019, Nature publisher. (C) Schematic illustration of improved PTT/PDT-driven cancer immunotherapy by combination with both HSP60 and NRF2 to inhibit immune-resistance caused by PTT and PDT. Reproduced with permission [162]. Copyright 2020, Elsevier Ltd.

Unlike metal PTAs (e.g., Au), some nonstoichiometric materials (e.g., CoWO_{4-x}) under a single wavelength light irradiation showed both PDT and PTT properties through the synchronous generation of ROS as well as hyperthermia [162]. In addition, these biomaterials have multimodal imaging abilities due to the presence of tungsten elements, which make them excellent PA agents [162]. Taking these advantages, Liu et al. designed a multifunctional CoWO_{4-x} nanoplatform to enhance the PDT/PTT immunotherapy, in which the surface of CoWO_{4-x} NPs was modified with hydrophilic polymers to improve the biocompatibility and stability (**Figure 10C**) [162]. With tungsten elements and NIR absorption properties, CoWO_{4-x} NPs showed excellent PA and CT imaging, which helped to better monitor the *in vivo* dynamics of NPs. Furthermore, the nonstoichiometric CoWO_{4-x} NPs under laser irradiation induced both PDT and PTT, resulting in increased HMGB1 expression and CRT exposure. However, the ICD induced by phototherapy (PDT-PTT) provided a disappointing therapeutic effect. They found that phototherapy induced the overexpression of immunosuppressive agents (NRF2 and HSP60). Therefore, CoWO_{4-x} nanoplatform combined with specific inhibitors of immunosuppressive agents (ML385 and etoposide) realized a synergistic therapeutic effect of phototherapy and immunotherapy [162]. Recently, organic semiconducting polymer nanoplatforms (OSPNs) have drawn much more attention. This is because the OSPNs not only induce PDT and PTT by converting optical energy into ROS and hyperthermia, but also exhibit some unique advantages, including excellent biocompatibility, good photostability, tunable optical properties, and large absorption coefficients [166-168]. For example, Pu et al. developed a prodrug-based OSPN consisting of NLG919-conjugated semiconducting polymer NPs via ¹O₂ cleavable linkers to achieve an accurate phototherapy-induced immunotherapy [164, 169]. This OSPN under laser irradiation induced synergistic PDT and PTT by producing ¹O₂ and hyperthermia to ablate tumors. Subsequently, the generated ¹O₂ selectively cleaved the ¹O₂-responsive linkers to accelerate the release of NLG919. More importantly, the phototherapy induced ICD to significantly enhance the proliferation of CTLs, and then the locally released NLG919 restored the activation of CTLs by inhibiting the IDO pathway. As a result, the OSPN achieved synergistic antitumor immunotherapy against malignant tumors [164]. Bioinspired polydopamine (PDA) prepared by the autoxidation polymerization of dopamine has many properties, including excellent photothermal conversion

efficiency, strong adhesive property, and good biocompatibility [170]. Thanks to these properties, Yan et al. designed PDA-coated UCNs loaded with Ce6 to combine PDT and PTT to induce immunotherapy against disseminated tumors [165]. Compared to single approach (PDT or PTT), they found that the synergistic phototherapy promoted TAA release and DC maturation, inducing a strong immune response. Moreover, this synergistic phototherapy also recruited macrophages and B cells, eliciting an innate immune response. Furthermore, this nanoplatform in combination with αPD-1 activated the proliferation of memory T cells to prevent tumor from relapse and metastasis [165].

4. Conclusions and future perspectives

Although cancer immunotherapy has achieved numerous clinical success, patients with cancer have a low response rate. Progressive nanomedicines significantly improve the efficacy of PDT by overcoming the main challenges, including ACQ, tumor hypoxia, and off-target effects. As a result, the facilitated PDT significantly increase the potential to induce immune responses, thereby further driving systemic cancer immunotherapy. We reviewed several emerging nanomedicines in the skillful incorporation of PDT with immunotherapy to better understand the intrinsic advantages of combinatorial therapy. Moreover, nanoparticle-based conventional cancer treatments (e.g., PTT and chemotherapy) can also induce ICD via sequential changes, achieving desirable synergistic effects in combination with PDT to initiate intense immune responses.

Despite the development of nanomedicines in PDT-driven cancer immunotherapy, there are still several challenges and opportunities in the following areas. First, the effective immune response for immunotherapy urgently needs the simultaneous activation of multiple immune signaling pathways [77]. Therefore, it still requires advanced biomaterials to optimize multifunctional noncarriers for the codelivery of various immunomodulators to specific cells. Second, components of polymer-based nanomedicines and inorganic nanomaterials usually exhibit poor biodegradability, significantly limiting their clinical translation [171, 172]. Hence, small molecule based self-assembled nanomedicines with well-defined chemical structures are suitable for clinical translation [173-175]. Third, new strategies (e.g., ACT) combined with PDT can provide the opportunity to enhance the immune response by engineering immune cells. Moreover, nanosized extracellular vesicles derived from immune cells can serve as excellent biocompatible carriers with good tumor-targeting ability [77, 173]. Fourth, ferroptosis, a

nonapoptotic programmed cell death modality, not only supplies O₂ to increase the efficacy of PDT, but also produces ROS to induce immune responses [176]. More importantly, based on their intrinsic connections of O₂ and ROS, a combination of PDT and ferroptosis will achieve a synergistic effect to initiate strong immune response. In addition, PDT can activate T lymphocytes to release IFN-γ, which will facilitate the ferroptosis-related lipid peroxidation to further improve the ICD effect [177-180]. Therefore, novel nanoplatforms developed by the rational integration of PDT, ferroptosis, and immunotherapy have attracted much attention for cancer treatment [180]. Finally, in-depth exploration of the relationship between PDT and cancer immunotherapy is still needed, and more advanced nanomedicines will boost the effectiveness and safety of combinational cancer immunotherapy [181].

Acknowledgements

We thank the National Natural Science Foundation of China (No. 22074012), Doctoral Scientific Research Launching Fund Project of Liaoning province (No. 2021-BS-104), NSFC-Liaoning Joint Fund Key Program (No. U20A20413) and China Postdoctoral Science Foundation (No. 2021MD703908).

Competing Interests

The authors have declared that no competing interest exists.

References

- Holohan C, Van Schaeybroeck S, Longley DB, Johnston PG. Cancer drug resistance: an evolving paradigm. *Nat Rev Cancer*. 2013; 13: 714-26.
- Vanneman M, Dranoff G. Vanneman M, Dranoff GCombining immunotherapy and targeted therapies in cancer treatment. *Nat Rev Cancer* 12: 237-251. *Nat Rev Cancer*. 2012; 12: 237-51.
- Ribas A, Wolchok JD. Cancer immunotherapy using checkpoint blockade. *Science*. 2018; 359: 1350.
- Riley RS, June CH, Langer R, Mitchell MJ. Delivery technologies for cancer immunotherapy. *Nat Rev Drug Discov*. 2019; 18: 175-96.
- Khalil DN, Smith EL, Brentjens RJ, Wolchok JD. The future of cancer treatment: immunomodulation, CARs and combination immunotherapy. *Nat Rev Clin Oncol*. 2016; 13: 394.
- Li Q, Zhao ZP, Qin XH, Zhang MZ, Du Q, Li ZH, et al. A Checkpoint-Regulatable Immune Niche Created by Injectable Hydrogel for Tumor Therapy. *Adv Funct Mater*. 2021; 31: 13.
- Schadendorf D, Hodi FS, Robert C, Weber JS, Margolin K, Hamid O, et al. Pooled Analysis of Long-Term Survival Data From Phase II and Phase III Trials of Ipilimumab in Unresectable or Metastatic Melanoma. *J Clin Oncol*. 2015; 33: 1889-94.
- Zou W, Wolchok JD, Chen L. PD-L1 (B7-H1) and PD-1 pathway blockade for cancer therapy: Mechanisms, response biomarkers, and combinations. *Sci Transl Med*. 2016; 8: 328rv4.
- Kim TK, Herbst RS, Chen L. Defining and Understanding Adaptive Resistance in Cancer Immunotherapy. *Trends Immunol*. 2018; 39: 624-31.
- Wang C, Wang J, Zhang X, Yu S, Wen D, Hu Q, et al. *In situ* formed reactive oxygen species-responsive scaffold with gemcitabine and checkpoint inhibitor for combination therapy. *Sci Transl Med*. 2018; 10: eaan3682.
- Binniewies M, Roberts EW, Kersten K, Chan V, Fearon DF, Merad M, et al. Understanding the tumor immune microenvironment (TIME) for effective therapy. *Nat Med*. 2018; 24: 541-50.
- Lucky SS, Soo KC, Zhang Y. Nanoparticles in photodynamic therapy. *Chem Rev*. 2015; 115: 1990-2042.
- Chen J, Fan T, Xie Z, Zeng Q, Xue P, Zheng T, et al. Advances in nanomaterials for photodynamic therapy applications: Status and challenges. *Biomaterials*. 2020; 237: 119827.
- Zhou YX, Ren XM, Hou ZS, Wang NN, Jiang Y, Luan YX. Engineering a photosensitizer nanoplateform for amplified photodynamic immunotherapy via tumor microenvironment modulation. *Nanoscale Horiz*. 2021; 6: 120-31.
- Qin XH, Zhang MZ, Hu X, Du Q, Zhao ZP, Jiang Y, et al. Nanoengineering of a newly designed chlorin e6 derivative for amplified photodynamic therapy via regulating lactate metabolism. *Nanoscale*. 2021; 13: 11953-62.
- Zhang MZ, Qin XH, Xu W, Wang YB, Song YM, Garg S, et al. Engineering of a dual-modal phototherapeutic nanoplateform for single NIR laser-triggered tumor therapy. *J Colloid Interface Sci*. 2021; 594: 493-501.
- Zhang J, Wang NN, Li Q, Zhou YX, Luan YX. A two-pronged photodynamic nanodrug to prevent metastasis of basal-like breast cancer. *Chem Commun*. 2021; 57: 2305-8.
- Nam J, Son S, Park KS, Zou W, Shea LD, Moon JJJNRM. Cancer nanomedicine for combination cancer immunotherapy. *Nat Rev Mater*. 2019; 4: 398-414.
- Shafi-Muthana M, McIntyre C, Sisley K, Rennie I, Murray A. Dead or alive: immunogenicity of human melanoma cells when presented by dendritic cells. *Cancer Res*. 2000; 60: 6441-7.
- Srivastava P. Roles of heat-shock proteins in innate and adaptive immunity. *Nat Rev Immunol*. 2002; 2: 185-94.
- Kim D, Lee S, Na K. Immune Stimulating Antibody-Photosensitizer Conjugates via Fc-Mediated Dendritic Cell Phagocytosis and Phototriggered Immunogenic Cell Death for KRAS-Mutated Pancreatic Cancer Treatment. *Small*. 2021; 17: e2006650.
- Min Y, Roche KC, Tian S, Eblan MJ, McKinnon KP, Caster JM, et al. Antigen-capturing nanoparticles improve the abscopal effect and cancer immunotherapy. *Nat Nanotechnol*. 2017; 12: 877-82.
- Korbelik M. Induction of tumor immunity by photodynamic therapy. *J Clin Laser Med Surg*. 1996; 14: 329-34.
- Duan X, Chan C, Lin W. Nanoparticle-Mediated Immunogenic Cell Death Enables and Potentiates Cancer Immunotherapy. *Angew Chem Int Ed Engl*. 2019; 58: 670-80.
- Gellén E, Fidrus E, Péter M, Szegedi A, Emri G, Remenyik É. Immunological effects of photodynamic therapy in the treatment of actinic keratosis and squamous cell carcinoma. *Photodiagnosis Photodyn Ther*. 2018; 24: 342-8.
- Yang Y, Zhu W, Feng L, Chao Y, Yi X, Dong Z, et al. G-Quadruplex-Based Nanoscale Coordination Polymers to Modulate Tumor Hypoxia and Achieve Nuclear-Targeted Drug Delivery for Enhanced Photodynamic Therapy. *Nano Lett*. 2018; 18: 6867-75.
- Cao H, Wang L, Yang Y, Li J, Qi Y, Li Y, et al. An Assembled Nanocomplex for Improving both Therapeutic Efficiency and Treatment Depth in Photodynamic Therapy. *Angew Chem Int Ed Engl*. 2018; 57: 7759-63.
- Tian J, Xiao C, Huang B, Wang C, Zhang W. Janus macromolecular brushes for synergistic cascade-amplified photodynamic therapy and enhanced chemotherapy. *Acta Biomater*. 2020; 101: 495-506.
- Wang M, Zhai Y, Ye H, Lv Q, Sun B, Luo C, et al. High Co-loading Capacity and Stimuli-Responsive Release Based on Cascade Reaction of Self-Destructive Polymer for Improved Chemo-Photodynamic Therapy. *ACS Nano*. 2019; 13: 7010-23.
- Deng G, Sun Z, Li S, Peng X, Li W, Zhou L, et al. Cell-Membrane Immunotherapy Based on Natural Killer Cell Membrane Coated Nanoparticles for the Effective Inhibition of Primary and Abscopal Tumor Growth. *ACS Nano*. 2018; 12: 12096-108.
- Liu Z, Xie Z, Li W, Wu X, Jiang X, Li G, et al. Photodynamic immunotherapy of cancers based on nanotechnology: recent advances and future challenges. *J Nanobiotechnology*. 2021; 19: 160.
- Sharma P, Hu-Lieskovsky S, Wargo JA, Ribas A. Primary, Adaptive, and Acquired Resistance to Cancer Immunotherapy. *Cell*. 2017; 168: 707-23.
- Wu X, Yang H, Chen X, Gao J, Duan Y, Wei D, et al. Nano-herb medicine and PDT induced synergistic immunotherapy for colon cancer treatment. *Biomaterials*. 2021; 269: 120654.
- Kroemer G, Galluzzi L, Kepp O, Zitvogel L. Immunogenic cell death in cancer therapy. *Annu Rev Immunol*. 2013; 31: 51-72.
- Galluzzi L, Buqué A, Kepp O, Zitvogel L, Kroemer G. Immunogenic cell death in cancer and infectious disease. *Nat Rev Immunol*. 2017; 17: 97-111.
- Yang W, Zhang F, Deng H, Lin L, Wang S, Kang F, et al. Smart Nanovesicle-Mediated Immunogenic Cell Death through Tumor Microenvironment Modulation for Effective Photodynamic Immunotherapy. *ACS Nano*. 2020; 14: 620-31.
- Fan W, Huang P, Chen X. Overcoming the Achilles' heel of photodynamic therapy. *Chem Soc Rev*. 2016; 45: 6488-519.
- McDonald PC, Chafe SC, Dedhar S. Overcoming Hypoxia-Mediated Tumor Progression: Combinatorial Approaches Targeting pH Regulation, Angiogenesis and Immune Dysfunction. *Front Cell Dev Biol*. 2016; 4: 27.
- Wang H, Tang Y, Fang Y, Zhang M, Wang H, He Z, et al. Reprogramming Tumor Immune Microenvironment (TIME) and Metabolism via Biomimetic Targeting Codelivery of Shikonin/JQ1. *Nano Lett*. 2019; 19: 2935-44.
- Zhang Y, Liao Y, Tang Q, Lin J, Huang P. Biomimetic Nanoemulsion for Synergistic Photodynamic-Immunotherapy Against Hypoxic Breast Tumor. *Angew Chem Int Ed Engl*. 2021; 60: 10647-53.
- Liang R, Liu L, He H, Chen Z, Han Z, Luo Z, et al. Oxygen-boosted immunogenic photodynamic therapy with gold nanocages@manganese

- dioxide to inhibit tumor growth and metastases. *Biomaterials.* 2018; 177: 149-60.
42. Liu Y, Pan Y, Cao W, Xia F, Liu B, Niu J, et al. A tumor microenvironment responsive biodegradable CaCO(3)/MnO(2)- based nanoplatform for the enhanced photodynamic therapy and improved PD-L1 immunotherapy. *Theranostics.* 2019; 9: 6867-84.
 43. Chen Z, Liu L, Liang R, Luo Z, He H, Wu Z, et al. Bioinspired Hybrid Protein Oxygen Nanocarrier Amplified Photodynamic Therapy for Eliciting Anti-tumor Immunity and Abscopal Effect. *ACS Nano.* 2018; 12: 8633-45.
 44. Xing L, Gong JH, Wang Y, Zhu Y, Huang ZJ, Zhao J, et al. Hypoxia alleviation-triggered enhanced photodynamic therapy in combination with IDO inhibitor for preferable cancer therapy. *Biomaterials.* 2019; 206: 170-82.
 45. Wang H, Han X, Dong Z, Xu J, Wang J, Liu Z. Hyaluronidase with pH-responsive Dextran Modification as an Adjuvant Nanomedicine for Enhanced Photodynamic-Immunotherapy of Cancer. *Adv Funct Mater.* 2019; 29: 1902440.
 46. Mai X, Zhang Y, Fan H, Song W, Chang Y, Chen B, et al. Integration of immunogenic activation and immunosuppressive reversion using mitochondrial-respiration-inhibited platelet-mimicking nanoparticles. *Biomaterials.* 2020; 232: 119699.
 47. Chung CH, Lu KY, Lee WC, Hsu WJ, Lee WF, Dai JZ, et al. Fucoidan-based, tumor-activated nanoplatform for overcoming hypoxia and enhancing photodynamic therapy and antitumor immunity. *Biomaterials.* 2020; 257: 120227.
 48. Li Y, Wen T, Zhao R, Liu X, Ji T, Wang H, et al. Localized electric field of plasmonic nanoplatform enhanced photodynamic tumor therapy. *ACS Nano.* 2014; 8: 11529-42.
 49. Pang B, Yang X, Xia Y. Putting gold nanocages to work for optical imaging, controlled release and cancer theranostics. *Nanomedicine-UK.* 2016; 11: 1715-28.
 50. Jin L, Shen S, Huang Y, Li D, Yang X. Corn-like Au/Ag nanorod-mediated NIR-II photothermal/photodynamic therapy potentiates immune checkpoint antibody efficacy by reprogramming the cold tumor microenvironment. *Biomaterials.* 2021; 268: 120582.
 51. Song J, Yang X, Jacobson O, Huang P, Sun X, Lin L, et al. Ultrasmall Gold Nanorod Vesicles with Enhanced Tumor Accumulation and Fast Excretion from the Body for Cancer Therapy. *Adv Mater.* 2015; 27: 4910-7.
 52. Zhou TJ, Xing L, Fan YT, Cui PF, Jiang HL. Inhibition of breast cancer proliferation and metastasis by strengthening host immunity with a prolonged oxygen-generating phototherapy hydrogel. *J Control Release.* 2019; 309: 82-93.
 53. He YC, Cong C, He YQ, Hao ZN, Li CH, Wang S, et al. Tumor hypoxia relief overcomes multidrug resistance and immune inhibition for self-enhanced photodynamic therapy. *Chem Eng J.* 2019; 375: 122079.
 54. Meng Z, Zhou X, Xu J, Han X, Dong Z, Wang H, et al. Light-Triggered *In Situ* Gelation to Enable Robust Photodynamic-Immunotherapy by Repeated Stimulation. *Adv Mater.* 2019; 31: e1900927.
 55. Fan W, Bu W, Shen B, He Q, Cui Z, Liu Y, et al. Intelligent MnO₂ Nanosheets Anchored with Upconversion Nanopropes for Concurrent pH-/H₂O₂-Responsive UCL Imaging and Oxygen-Elevated Synergistic Therapy. *Adv Mater.* 2015; 27: 4155-61.
 56. Song M, Liu T, Shi C, Zhang X, Chen X. Bioconjugated Manganese Dioxide Nanoparticles Enhance Chemotherapy Response by Priming Tumor-Associated Macrophages toward M1-like Phenotype and Attenuating Tumor Hypoxia. *ACS Nano.* 2016; 10: 633-47.
 57. Li W, Yang J, Luo L, Jiang M, Qin B, Yin H, et al. Targeting photodynamic and photothermal therapy to the endoplasmic reticulum enhances immunogenic cancer cell death. *Nat Commun.* 2019; 10: 3349.
 58. Tao D, Feng L, Chao Y, Liang C, Song X, Wang H, et al. Covalent Organic Polymers Based on Fluorinated Porphyrin as Oxygen Nanoshuttles for Tumor Hypoxia Relief and Enhanced Photodynamic Therapy. *Adv Funct Mater.* 2018; 28: 1804901.
 59. Valkenburg KC, de Groot AE, Pienta KJ. Targeting the tumour stroma to improve cancer therapy. *Nat Rev Clin Oncol.* 2018; 15: 366-81.
 60. Shiga K, Hara M, Nagasaki T, Sato T, Takahashi H, Takeyama H. Cancer-Associated Fibroblasts: Their Characteristics and Their Roles in Tumor Growth. *Cancers.* 2015; 7: 2443-58.
 61. Bonnans C, Chou J, Werb Z. Remodelling the extracellular matrix in development and disease. *Nat Rev Mol Cell Biol.* 2014; 15: 786-801.
 62. Yang C, Fu Y, Huang C, Hu D, Zhou K, Hao Y, et al. Chlorin e6 and CRISPR-Cas9 dual-loading system with deep penetration for a synergistic tumoral photodynamic-immunotherapy. *Biomaterials.* 2020; 255: 120194.
 63. Xiong W, Qi L, Jiang N, Zhao Q, Chen L, Jiang X, et al. Metformin Liposome-Mediated PD-L1 Downregulation for Amplifying the Photodynamic Immunotherapy Efficacy. *ACS Appl Mater Interfaces.* 2021; 13: 8026-41.
 64. Frangioni JV. *In vivo* near-infrared fluorescence imaging. *Curr Opin Chem Biol.* 2003; 7: 626-34.
 65. Dong H, R.X. W, Liu JQ, Huang Q, Zhou Y, Hu YQ. Advances in cancer photodynamic therapy. *Journal of China Pharmaceutical University.* 2016; 47: 377-87.
 66. Wang C, Cheng L, Liu Z. Upconversion Nanoparticles for Photodynamic Therapy and Other Cancer Therapeutics. *Theranostics.* 2013; 3: 317-30.
 67. Ai X, Hu M, Wang Z, Lyu L, Zhang W, Li J, et al. Enhanced Cellular Ablation by Attenuating Hypoxia Status and Reprogramming Tumor-Associated Macrophages via NIR Light-Responsive Upconversion Nanocrystals. *Biconjup Chem.* 2018; 29: 928-38.
 68. Xu J, Xu L, Wang C, Yang R, Zhuang Q, Han X, et al. Near-Infrared-Triggered Photodynamic Therapy with Multitasking Upconversion Nanoparticles in Combination with Checkpoint Blockade for Immunotherapy of Colorectal Cancer. *ACS Nano.* 2017; 11: 4463-74.
 69. Chen Q, Xu L, Liang C, Wang C, Peng R, Liu Z. Photothermal therapy with immune-adjuvant nanoparticles together with checkpoint blockade for effective cancer immunotherapy. *Nat Commun.* 2016; 7: 13193.
 70. Lan G, Ni K, Lin W. Nanoscale Metal-Organic Frameworks for Phototherapy of Cancer. *Coord Chem Rev.* 2019; 379: 65-81.
 71. Ni K, Lan G, Lin W. Nanoscale Metal-Organic Frameworks Generate Reactive Oxygen Species for Cancer Therapy. *ACS Cent Sci.* 2020; 6: 861-8.
 72. Anderson SL, Boyd PG, Gladyska A, Nguyen TN, Palgrave RG, Kubicki D, et al. Nucleobase pairing and photodimerization in a biologically derived metal-organic framework nanoreactor. *Nat Commun.* 2019; 10: 1612.
 73. Cai Z, Xin F, Wei Z, Wu M, Lin X, Du X, et al. Photodynamic Therapy Combined with Antihypoxic Signaling and CpG Adjuvant as an *In Situ* Tumor Vaccine Based on Metal-Organic Framework Nanoparticles to Boost Cancer Immunotherapy. *Adv Health Mater.* 2020; 9: e1900996.
 74. Liu WL, Zou MZ, Liu T, Zeng JY, Li X, Yu WY, et al. Expandable Immunotherapeutic Nanoplatforms Engineered from Cytomembranes of Hybrid Cells Derived from Cancer and Dendritic Cells. *Adv Mater.* 2019; 31: e1900499.
 75. Lu K, He C, Guo N, Chan C, Ni K, Weichselbaum RR, et al. Chlorin-Based Nanoscale Metal-Organic Framework Systemically Rejects Colorectal Cancers via Synergistic Photodynamic Therapy and Checkpoint Blockade Immunotherapy. *J Am Chem Soc.* 2016; 138: 12502-10.
 76. Zeng JY, Zou MZ, Zhang M, Wang XS, Zeng X, Cong H, et al. π-Extended Benzoporphyrin-Based Metal-Organic Framework for Inhibition of Tumor Metastasis. *ACS Nano.* 2018; 12: 4630-40.
 77. Caster JM, Callaghan C, Seyedin SN, Henderson K, Sun B, Wang AZ. Optimizing Advances in Nanoparticle Delivery for Cancer Immunotherapy. *Adv Drug Deliv Rev.* 2019; 144: 3-15.
 78. Musette S, Huang L. Nanoparticle-Mediated Remodeling of the Tumor Microenvironment to Enhance Immunotherapy. *ACS Nano.* 2018; 12: 11740-55.
 79. Munn DH, Mellor AL. IDO in the Tumor Microenvironment: Inflammation, Counter-Regulation, and Tolerance. *Trends Immunol.* 2016; 37: 193-207.
 80. Ni K, Luo T, Lan G, Culbert A, Song Y, Wu T, et al. A Nanoscale Metal-Organic Framework to Mediate Photodynamic Therapy and Deliver CpG Oligodeoxynucleotides to Enhance Antigen Presentation and Cancer Immunotherapy. *Angew Chem Int Ed Engl.* 2020; 59: 1108-12.
 81. Yang G, Phua SZF, Lim WQ, Zhang R, Feng L, Liu G, et al. A Hypoxia-Responsive Albumin-Based Nanosystem for Deep Tumor Penetration and Excellent Therapeutic Efficacy. *Adv Mater.* 2019; 31: 1901513.
 82. Liu D, Chen B, Mo Y, Wang Z, Qi T, Zhang Q, et al. Redox-Activated Porphyrin-Based Liposome Remote-Loaded with Indoleamine 2,3-Dioxygenase (IDO) Inhibitor for Synergistic Photoimmunotherapy through Induction of Immunogenic Cell Death and Blockage of IDO Pathway. *Nano Lett.* 2019; 19: 6964-76.
 83. Sun X, Cao Z, Mao K, Wu C, Chen H, Wang J, et al. Photodynamic therapy produces enhanced efficacy of antitumor immunotherapy by simultaneously inducing intratumoral release of sorafenib. *Biomaterials.* 2020; 240: 119845.
 84. Im S, Lee J, Park D, Park A, Kim YM, Kim WJ. Hypoxia-Triggered Transforming Immunomodulator for Cancer Immunotherapy via Photodynamically Enhanced Antigen Presentation of Dendritic Cell. *ACS Nano.* 2019; 13: 476-88.
 85. Volk T, Jähde E, Fortmeyer HP, Glüsenkamp KH, Rajewsky MF. pH in human tumour xenografts: effect of intravenous administration of glucose. *Br J Cancer.* 1993; 68: 492-500.
 86. Wang D, Wang T, Liu J, Yu H, Jiao S, Feng B, et al. Acid-Activatable Versatile Micelleplexes for PD-L1 Blockade-Enhanced Cancer Photodynamic Immunotherapy. *Nano Lett.* 2016; 16: 5503-13.
 87. Yang G, Xu L, Xu J, Zhang R, Song G, Chao Y, et al. Smart Nanoreactors for pH-Responsive Tumor Homing, Mitochondria-Targeting, and Enhanced Photodynamic-Immunotherapy of Cancer. *Nano Lett.* 2018; 18: 2475-84.
 88. Stehle G, Sinn H, Wunder A, Schrenk HH, Stewart JC, Hartung G, et al. Plasma protein (albumin) catabolism by the tumor itself-implications for tumor metabolism and the genesis of cachexia. *Crit Rev Oncol Hematol.* 1997; 26: 77-100.
 89. Lu J, Liu X, Liao YP, Salazar F, Sun B. Nano-enabled pancreas cancer immunotherapy using immunogenic cell death and reversing immunosuppression. *Nat Commun.* 2017; 8: 1811.
 90. Song W, Kuang J, Li C-X, Zhang M, Zheng D, Zeng X, et al. Enhanced Immunotherapy Based on Photodynamic Therapy for Both Primary and Lung Metastasis Tumor Eradication. *ACS Nano.* 2018; 12: 1978-89.
 91. Zheng Y-R, Suntharalingam K, Johnstone TC, Yoo H, Lin W, Brooks JG, et al. Pt(IV) Prodrugs Designed to Bind Non-Covalently to Human Serum Albumin for Drug Delivery. *J Am Chem Soc.* 2014; 136: 8790-8.
 92. Tian J, Ding L, Xu H-J, Shen Z, Ju H, Jia L, et al. Cell-specific and pH-activatable rubryin-loaded nanoparticles for highly selective near-infrared photodynamic therapy against cancer. *J Am Chem Soc.* 2013; 135: 18850-8.

93. Hu X, Hou B, Xu Z, Saeed M, Sun F, Gao Z, et al. Supramolecular Prodrug Nanovectors for Active Tumor Targeting and Combination Immunotherapy of Colorectal Cancer. *Adv Sci.* 2020; 7: 1903332.
94. Su J, Sun H, Meng Q, Zhang P, Yin Q, Li Y. Enhanced Blood Suspensibility and Laser-Activated Tumor-specific Drug Release of Theranostic Mesoporous Silica Nanoparticles by Functionalizing with Erythrocyte Membranes. *Theranostics.* 2017; 7: 523-37.
95. Shen D, Yang J, Li X, Zhou L, Zhang R, Li W, et al. Biphase stratification approach to three-dimensional dendritic biodegradable mesoporous silica nanospheres. *Nano Lett.* 2014; 14: 923-32.
96. Xu C, Nam J, Hong H, Xu Y, Moon JJ. Positron Emission Tomography-Guided Photodynamic Therapy with Biodegradable Mesoporous Silica Nanoparticles for Personalized Cancer Immunotherapy. *ACS Nano.* 2019; 13: 12148-61.
97. Jin H, Zhu T, Huang X, Sun M, Li H, Zhu X, et al. ROS-responsive nanoparticles based on amphiphilic hyperbranched polyphosphoester for drug delivery: Light-triggered size-reducing and enhanced tumor penetration. *Biomaterials.* 2019; 211: 68-80.
98. Zheng M, Liu Y, Wang Y, Zhang D, Zou Y, Ruan W, et al. ROS-Responsive Polymeric siRNA Nanomedicine Stabilized by Triple Interactions for the Robust Glioblastoma Combinational RNAi Therapy. *Adv Mater.* 2019; 31: e1903277.
99. Yang B, Wang K, Zhang D, Sun B, Ji B, Wei L, et al. Light-activatable dual-source ROS-responsive prodrug nanoplatform for synergistic chemo-photodynamic therapy. *Biomater Sci.* 2018; 6: 2965-75.
100. Vordermark D. Hypoxia-specific targets in cancer therapy: role of splice variants. *BMC Med.* 2010; 8: 45.
101. McKeown SR. Defining normoxia, physoxia and hypoxia in tumours-implications for treatment response. *Br J Radiol.* 2014; 87: 20130676.
102. Zhang F, Zhu G, Jacobson O, Liu Y, Chen K, Yu G, et al. Transformative Nanomedicine of an Amphiphilic Camptothecin Prodrug for Long Circulation and High Tumor Uptake in Cancer Therapy. *ACS Nano.* 2017; 11: 8838-48.
103. Li X, Jeon YH, Kwon N, Park JG, Guo T, Kim HR, et al. *In Vivo*-assembled phthalocyanine/albumin supramolecular complexes combined with a hypoxia-activated prodrug for enhanced photodynamic immunotherapy of cancer. *Biomaterials.* 2021; 266: 120430.
104. Liu J, Ai X, Cabral H, Liu J, Huang Y, Mi P. Tumor hypoxia-activated combinatorial nanomedicine triggers systemic antitumor immunity to effectively eradicate advanced breast cancer. *Biomaterials.* 2021; 273: 120847.
105. Blanco E, Shen H, Ferrari M. Principles of nanoparticle design for overcoming biological barriers to drug delivery. *Nat Biotechnol.* 2015; 33: 941-51.
106. Gawade PM, Shadish JA, Badeau BA, DeForest CA. Boolean Biomaterials: Logic-Based Delivery of Site-Specifically Modified Proteins from Environmentally Responsive Hydrogel Biomaterials (*Adv. Mater.* 33/2019). *Adv Mater.* 2019; 31: 1970237.
107. Badeau BA, Comerford MP, Arakawa CK, Shadish JA, DeForest CA. Engineered modular biomaterial logic gates for environmentally triggered therapeutic delivery. *Nat Chem.* 2018; 10: 251-8.
108. Hou B, Zhou L, Wang H, Saeed M, Wang D, Xu Z, et al. Engineering Stimuli-Activatable Boolean Logic Prodrug Nanoparticles for Combination Cancer Immunotherapy. *Adv Mater.* 2020; 32: e1907210.
109. Gai Shili, Yang Guixin, Piaoping He, et al. Recent advances in functional nanomaterials for light-triggered cancer therapy. *Nano Today.* 2018; 19: 146-187.
110. Zhou Z, Song J, Nie L, Chen X. Reactive oxygen species generating systems meeting challenges of photodynamic cancer therapy. *Chem Soc Rev.* 2016; 45:6597-6626.
111. Moan J, Berg K. The photodegradation of porphyrins in cells can be used to estimate the lifetime of singlet oxygen. *Photochem Photobiol.* 1991; 53: 549-53.
112. Vinklárek IS, Scholz M, Dědick R, Hála J. Singlet oxygen feedback delayed fluorescence of protoporphyrin IX in organic solutions. *Photochem Photobiol Sci.* 2017; 16: 507-18.
113. Verfaillie T, Garg AD, Agostinis P. Targeting ER stress induced apoptosis and inflammation in cancer. *Cancer Lett.* 2013; 332: 249-64.
114. Cheng H, Zheng RR, Fan GL, Fan JH, Zhao LP, Jiang XY, et al. Mitochondria and plasma membrane dual-targeted chimeric peptide for single-agent synergistic photodynamic therapy. *Biomaterials.* 2019; 188: 1-11.
115. Huang H, Yu B, Zhang P, Huang J, Chen Y, Gasser G, et al. Highly Charged Ruthenium(II) Polypyridyl Complexes as Lysosome-Localized Photosensitizers for Two-Photon Photodynamic Therapy. *Angew Chem Int Ed Engl.* 2015; 54: 14049-52.
116. Yu Z, Pan W, Li N, Tang B. A nuclear targeted dual-photosensitizer for drug-resistant cancer therapy with NIR activated multiple ROS. *Chem Sci.* 2016; 7: 4237-44.
117. Liu LH, Qiu WX, Zhang YH, Li B, Zhang C, Gao F, et al. A Charge Reversible Self-Delivery Chimeric Peptide with Cell Membrane-Targeting Properties for Enhanced Photodynamic Therapy. *Adv Funct Mater.* 2017; 27: 1700220.1-15.
118. Deng H, Zhou Z, Yang W, Lin LS, Wang S, Niu G, et al. Endoplasmic Reticulum Targeting to Amplify Immunogenic Cell Death for Cancer Immunotherapy. *Nano Lett.* 2020; 20: 1928-33.
119. Peng N, Yu H, Yu W, Yang M, Chen H, Zou T, et al. Sequential-targeting nanocarriers with pH-controlled charge reversal for enhanced mitochondria-located photodynamic-immunotherapy of cancer. *Acta Biomater.* 2020; 105: 223-38.
120. Zhang C, Gao F, Wu W, Qiu WX, Zhang L, Li R, et al. Enzyme-Driven Membrane-Targeted Chimeric Peptide for Enhanced Tumor Photodynamic Immunotherapy. *ACS Nano.* 2019; 13: 11249-62.
121. Kessel D, Reiners JJ. Apoptosis and Autophagy After Mitochondrial or Endoplasmic Reticulum Photodamage. *Photochem Photobiol.* 2007; 83: 1024-8.
122. Sang W, Zhang Z, Dai Y, Chen X. Recent advances in nanomaterial-based synergistic combination cancer immunotherapy. *Chem Soc Rev.* 2019; 48: 3771-810.
123. Spang A. The endoplasmic reticulum-the caring mother of the cell. *Curr Opin Cell Biol.* 2018; 53: 92-6.
124. Galluzzi L, Kepp O, Kroemer G. Enlightening the impact of immunogenic cell death in photodynamic cancer therapy. *EMBO J.* 2012; 31: 1055-7.
125. Gomes-da-Silva LC, Zhao L, Bezu L, Zhou H, Sauvat A, Liu P, et al. Photodynamic therapy with rapamycin targets the endoplasmic reticulum and Golgi apparatus. *EMBO J.* 2018; 37: e98354.
126. Sabharwal SS, Schumacker PT. Mitochondrial ROS in cancer: initiators, amplifiers or an Achilles' heel? *Nat Rev Cancer.* 2014; 14: 709-21.
127. Fulda S, Galluzzi L, Kroemer G. Targeting mitochondria for cancer therapy. *Nat Rev Drug Discov.* 2010; 9: 447-64.
128. Lv W, Zhang Z, Zhang KY, Yang H, Liu S, Xu A, et al. A Mitochondria-Targeted Photosensitizer Showing Improved Photodynamic Therapy Effects Under Hypoxia. *Angew Chem Int Ed Engl.* 2016; 55: 9947-51.
129. Zhou W, Yu H, Zhang LJ, Wu B, Wang CX, Wang Q, et al. Redox-triggered activation of nanocarriers for mitochondria-targeting cancer chemotherapy. *Nanoscale.* 2017; 9: 17044-53.
130. Salnikov V, Lukyánenko YO, Frederick CA, Lederer WJ, Lukyánenko V. Probing the outer mitochondrial membrane in cardiac mitochondria with nanoparticles. *Biophys J.* 2007; 92: 1058-71.
131. Green DR, Ferguson T, Zitvogel L, Kroemer G. Immunogenic and tolerogenic cell death. *Nat Rev Immunol.* 2009; 9: 353-63.
132. Thompson CB. Apoptosis in the pathogenesis and treatment of disease. *Science.* 1995; 267: 1456-62.
133. Li SY, Qiu WX, Cheng H, Gao F, Cao FY, Zhang XZ. A Versatile Plasma Membrane Engineered Cell Vehicle for Contact-Cell-Enhanced Photodynamic Therapy. *Adv Funct Mater.* 2017; 27: 1604916.
134. Mahmoodi MM, Abate-Pella D, Pundsack TJ, Palsuledesai CC, Goff PC, Blank DA, et al. Nitrodibenzofuran: A One- and Two-Photon Sensitive Protecting Group That Is Superior to Brominated Hydroxycoumarin for Thiol Caging in Peptides. *J Am Chem Soc.* 2016; 138: 5848-59.
135. Weise K, Kapoor S, Denter C, Nikolaus J, Opitz N, Koch S, et al. Membrane-mediated induction and sorting of K-Ras microdomain signaling platforms. *J Am Chem Soc.* 2011; 133: 880-7.
136. Ahearn IM, Haigis K, Bar-Sagi D, Phillips MR. Regulating the regulator: post-translational modification of RAS. *Nat Rev Mol Cell Biol.* 2011; 13: 39-51.
137. Zhang R, Xing R, Jiao T, Ma K, Chen C, Ma G, et al. Carrier-Free, Chemophotodynamic Dual Nanodrugs via Self-Assembly for Synergistic Antitumor Therapy. *ACS Appl Mater Interfaces.* 2016; 8: 13262-9.
138. Zhao LP, Zheng RR, Huang JQ, Chen XY, Deng FA, Liu YB, et al. Self-Delivery Photo-Immune Stimulators for Photodynamic Sensitized Tumor Immunotherapy. *ACS Nano.* 2020; 14: 17100-17113.
139. Wang D, Wang T, Yu H, Feng B, Zhou L, Zhou F, et al. Engineering nanoparticles to locally activate T cells in the tumor microenvironment. *Sci Immunol.* 2019; 4: eaau6584.
140. Xu J, Yu S, Wang X, Qian Y, Wu W, Zhang S, et al. High Affinity of Chlorin e6 to Immunoglobulin G for Intraoperative Fluorescence Image-Guided Cancer Photodynamic and Checkpoint Blockade Therapy. *ACS Nano.* 2019; 13: 10242-60.
141. Wang H, Wang K, He L, Liu Y, Dong H, Li Y. Engineering antigen as photosensitiser nanocarrier to facilitate ROS triggered immune cascade for photodynamic immunotherapy. *Biomaterials.* 2020; 244: 119964.
142. Wang Y, Liu D, Zheng Q, Zhao Q, Zhang H, Ma Y, et al. Disulfide bond bridge insertion turns hydrophobic anticancer prodrugs into self-assembled nanomedicines. *Nano Lett.* 2014; 14: 5577-83.
143. Castano AP, Mroz P, Wu MX, Hamblin MR. Photodynamic therapy plus low-dose cyclophosphamide generates antitumor immunity in a mouse model. *Proc Natl Acad Sci U S A.* 2008; 105: 5495-500.
144. Yang W, Zhu G, Wang S, Yu G, Yang Z, Lin L, et al. *In Situ* Dendritic Cell Vaccine for Effective Cancer Immunotherapy. *ACS Nano.* 2019; 13: 3083-94.
145. Hu L, Cao Z, Ma L, Liu Z, Liao G, Wang J, et al. The potentiated checkpoint blockade immunotherapy by ROS-responsive nanocarrier-mediated cascade chemo-photodynamic therapy. *Biomaterials.* 2019; 223: 119469.
146. He C, Duan X, Guo N, Chan C, Poon C, Weichselbaum RR, et al. Core-shell nanoscale coordination polymers combine chemotherapy and photodynamic therapy to potentiate checkpoint blockade cancer immunotherapy. *Nat Commun.* 2016; 7: 12499.
147. Advani R, Flinn I, Popplewell L, Forero A, Bartlett NL, Ghosh N, et al. CD47 Blockade by Hu5F9-G4 and Rituximab in Non-Hodgkin's Lymphoma. *N Engl J Med.* 2018; 379: 1711-21.
148. Kershaw MH, Smyth MJ. Immunology. Making macrophages eat cancer. *Science.* 2013; 341: 41-2.
149. Sockolosky JT, Dougan M, Ingram JR, Ho CCM, Kauke MJ, Almo SC, et al. Durable antitumor responses to CD47 blockade require adaptive immune stimulation. *Proc Natl Acad Sci U S A.* 2016; 113: E2646-E54.
150. Zhou F, Feng B, Yu H, Wang D, Wang T, Ma Y, et al. Tumor Microenvironment-Activatable Prodrug Vesicles for Nanoenabled Cancer

- Chemoimmunotherapy Combining Immunogenic Cell Death Induction and CD47 Blockade. *Adv Mater.* 2019; 31: 1805888.
151. Feng B, Hou B, Xu Z, Saeed M, Yu H, Li Y. Self-Amplified Drug Delivery with Light-Inducible Nanocargoes to Enhance Cancer Immunotherapy. *Adv Mater.* 2019; 31: 1902960.
152. Cui D, Huang J, Zhen X, Li J, Jiang Y, Pu K. A Semiconducting Polymer Nano-prodrug for Hypoxia-Activated Photodynamic Cancer Therapy. *Angew Chem Int Ed Engl.* 2019; 58: 5920-4.
153. Jin CS, Lovell JF, Chen J, Zheng G. Ablation of hypoxic tumors with dose-equivalent photothermal, but not photodynamic, therapy using a nanostructured porphyrin assembly. *ACS Nano.* 2013; 7: 2541-50.
154. Huang H, Banerjee S, Qin K, Zhang P, Blacque O, Malcomson T, et al. Targeted photoredox catalysis in cancer cells. *Nat Chem.* 2019; 11: 1041-8.
155. Zhang M, Ye JJ, Xia Y, Wang ZY, Li CX, Wang XS, et al. Platelet-Mimicking Biotaxis Targeting Vasculature-Disrupted Tumors for Cascade Amplification of Hypoxia-Sensitive Therapy. *ACS Nano.* 2019; 13: 14230-40.
156. Liu M, Wang L, Zheng X, Liu S, Xie Z. Hypoxia-Triggered Nanoscale Metal-Organic Frameworks for Enhanced Anticancer Activity. *ACS Appl Mater Interfaces.* 2018; 10: 24638-47.
157. Shao Y, Liu B, Di Z, Zhang G, Sun LD, Li L, et al. Engineering of Upconverted Metal-Organic Frameworks for Near-Infrared Light-Triggered Combinational Photodynamic/Chemo-/Immunotherapy against Hypoxic Tumors. *J Am Chem Soc.* 2020; 142: 3939-46.
158. Chu KF, Dupuy DE. Thermal ablation of tumours: biological mechanisms and advances in therapy. *Nat Rev Cancer.* 2014; 14: 199-208.
159. Peng J, Xiao Y, Li W, Yang Q, Tan L, Jia Y, et al. Photosensitizer Micelles Together with IDO Inhibitor Enhance Cancer Photothermal Therapy and Immunotherapy. *Adv Sci.* 2018; 5: 1700891.
160. Zhang X, Tang J, Li C, Lu Y, Cheng L, Liu J. A targeting black phosphorus nanoparticle based immune cells nano-regulator for photodynamic/photothermal and photo-immunotherapy. *Bioact Mater.* 2021; 6: 472-89.
161. Chang M, Hou Z, Wang M, Wang M, Dang P, Liu J, et al. Cu(2) MoS(4) / Au Heterostructures with Enhanced Catalase-Like Activity and Photoconversion Efficiency for Primary/Metastatic Tumors Eradication by Phototherapy-Induced Immunotherapy. *Small.* 2020; 16: e1907146.
162. Liu H, Yang Q, Guo W, Lin H, Qu F. CoWO_{4-x}-based nanoplatform for multimode imaging and enhanced photothermal/photodynamic therapy. *Chem Eng J.* 2019; 385: 123979.
163. Wang Z, Zhang F, Shao D, Chang Z, Wang L, Hu H, et al. Janus Nanobullets Combine Photodynamic Therapy and Magnetic Hyperthermia to Potentiate Synergistic Anti-Metastatic Immunotherapy. *Adv Sci.* 2019; 6: 1901690.
164. Li J, Cui D, Huang J, He S, Yang Z, Zhang Y, et al. Organic Semiconducting Pro-nanostimulants for Near-Infrared Photoactivatable Cancer Immunotherapy. *Angew Chem Int Ed Engl.* 2019; 58: 12680-7.
165. Yan S, Zeng X, Tang Y, Liu BF, Wang Y, Liu X. Activating Antitumor Immunity and Antimetastatic Effect Through Polydopamine-Encapsulated Core-Shell Upconversion Nanoparticles. *Adv Mater.* 2019; 31: e1905825.
166. Wu C, Chiu DT. Highly fluorescent semiconducting polymer dots for biology and medicine. *Angew Chem Int Ed Engl.* 2013; 52: 3086-109.
167. Chen X, Li R, Liu Z, Sun K, Sun Z, Chen D, et al. Small Photoblinking Semiconductor Polymer Dots for Fluorescence Nanoscopy. *Adv Mater.* 2017; 29: 1604850.
168. Cui D, Li J, Zhao X, Pu K, Zhang R. Semiconducting Polymer Nanoreporters for Near-Infrared Chemiluminescence Imaging of Immunoactivation. *Adv Mater.* 2020; 32: e1906314.
169. Pu K, He S, Li J, Cheng P, Zeng Z, Zhang C, et al. Charge-Reversal Polymer Nano-modulators for Photodynamic Immunotherapy of Cancer. *Angew Chem Int Ed Engl.* 2021; 60: 19355-19363.
170. Cheng W, Zeng X, Chen H, Li Z, Zeng W, Mei L, et al. Versatile Polydopamine Platforms: Synthesis and Promising Applications for Surface Modification and Advanced Nanomedicine. *ACS Nano.* 2019; 13: 8537-65.
171. Liu X, Wang D, Zhang P, Li Y. Recent advances in nanosized drug delivery systems for overcoming the barriers to anti-PD immunotherapy of cancer. *Nano Today.* 2019; 29: 100801.
172. Cheng YJ, Hu JJ, Qin SY, Zhang AQ, Zhang XZ. Recent advances in functional mesoporous silica-based nanoplatforms for combinational photo-chemotherapy of cancer. *Biomaterials.* 2020; 232: 119738.
173. Zhang P, Zhai Y, Cai Y, Zhao Y, Li Y. Nanomedicine-Based Immunotherapy for the Treatment of Cancer Metastasis. *Adv Mater.* 2019; 31: e1904156.
174. Sun Y, Zhang Y, Gao Y, Wang P, He G, Blum NT, et al. Six Birds with One Stone: Versatile Nanoporphyrin for Single-Laser-Triggered Synergistic Phototheranostics and Robust Immune Activation. *Adv Mater.* 2020; 32: e2004481.
175. Zhang Y, Zhang W, Wang Y, Zhu J, Zhou M, Peng C, et al. Emerging nanotaxanes for cancer therapy. *Biomaterials.* 2021; 272: 120790.
176. Shan X, Li S, Sun B, Chen Q, Sun J, He Z, et al. Ferroptosis-driven nanotherapeutics for cancer treatment. *J Control Release.* 2020; 319: 322-32.
177. Zhu T, Shi L, Yu C, Dong Y, Qiu F, Shen L, et al. Ferroptosis Promotes Photodynamic Therapy: Supramolecular Photosensitizer-Inducer Nanodrug for Enhanced Cancer Treatment. *Theranostics.* 2019; 9: 3293-307.
178. Wang W, Green M, Choi JE, Gijón M, Kennedy PD, Johnson JK, et al. CD8(+) T cells regulate tumour ferroptosis during cancer immunotherapy. *Nature.* 2019; 569: 270-4.
179. Zhou SY, Zhen ZP, Paschall AV, Xue LJ, Yang XY, Blackwell AGB, et al. FAP-Targeted Photodynamic Therapy Mediated by Ferritin Nanoparticles Elicits an Immune Response against Cancer Cells and Cancer Associated Fibroblasts. *Adv Funct Mater.* 2021; 31: 2007017.
180. Song R, Li T, Ye J, Sun F, Hou B, Saeed M, et al. Acidity-Activatable Dynamic Nanoparticles Boosting Ferroptotic Cell Death for Immunotherapy of Cancer. *Adv Mater.* 2021; 33: e2101155.
181. Yang B, Gao J, Pei Q, Xu H, Yu H. Engineering Prodrug Nanomedicine for Cancer Immunotherapy. *Adv Sci.* 2020; 7: 2002365.